arXiv:1409.3990v2 [cond-mat.supr-con] 27 Mar 2015

Quasiparticle mass enhancement approaching optimal doping in a high-T_c superconductor

B. J. Ramshaw[1*], S. E. Sebastian[2], R. D. McDonald[1], James Day[3], B. S. Tan[2], Z. Zhu[1], J.B. Betts[1], Ruixing Liang[3,4], D. A. Bonn[3,4], W. N. Hardy[3,4], N. Harrison[1]

Feb 23, 2015

[1]Mail Stop E536, Los Alamos National Labs, Los Alamos, NM 87545
[2]Cavendish Laboratory, Cambridge University, JJ Thomson Avenue, Cambridge CB3 OHE, U.K
[3]Department of Physics and Astronomy, University of British Columbia, Vancouver V6T 1Z4, Canada
[4]Canadian Institute for Advanced Research, Toronto M5G 1Z8, Canada
[*]Corresponding author: bradramshaw@gmail.com

In the quest for superconductors with higher transition temperatures (T_c), one emerging motif is that electronic interactions favourable for superconductivity can be enhanced by fluctuations of a broken-symmetry phase. Recent experiments have suggested the existence of the requisite broken symmetry phase in the high-T_c cuprates, but the impact of such a phase on the ground-state electronic interactions has remained unclear. We use magnetic fields exceeding 90 tesla to access the underlying metallic state of the cuprate $YBa_2Cu_3O_{6+\delta}$ over a wide range of doping, and observe magnetic quantum oscillations that reveal a strong enhancement of the quasiparticle effective mass toward optimal doping. This mass enhancement results from increasing electronic interactions approaching optimal doping, and suggests a quantum-critical point at a hole doping of $p_{crit} \approx 0.18$.

In several classes of unconventional superconductors, such as the heavy fermions, organics, and iron pnictides, superconductivity has been linked to a quantum critical point (QCP). At a QCP, the system undergoes a phase transition and a change in symmetry at zero temperature; the associated quantum fluctuations enhance interactions, which can give rise to (or enhance) superconductivity [1, 2]. As the QCP is approached, these fluctuations produce stronger and stronger electronic correlations, resulting in an experimentally-observable enhancement of the electron effective mass [1, 3, 4, 5]. It is widely believed that spin fluctuations in the vicinity of an antiferromagnetic QCP are important for superconductivity in many heavy-fermion, organic, and pnictide superconductors [6, 2], leading to the ubiquitous phenomenon of a superconducting dome surrounding a QCP. The role of quantum-criticality in cuprate high-temperature superconductors is more controversial [7]: do the collapsing

experimental energy scales[8], enhanced superconducting properties (see Fig. 1), and evidence for a change in ground-state symmetry near optimal doping [9, 10, 11, 12, 13, 14, 15, 16] support the existence of strong fluctuations that are relevant to superconductivity [17, 18, 19, 2]? Alternative explanations for the phenomenology of the cuprate phase diagram focus on the physics of a lightly doped Mott insulator [7, 20], rather than a metal with competing broken-symmetry phases. Several investigations, both theoretical and experimental, suggest that competing order is present in the cuprates, and is associated with the charge (rather than spin) degree of freedom (such as charge density wave order, orbital current order, or nematicity, see Fig. 1) [12, 15, 16, 17, 18, 21, 22, 23, 24, 25, 26, 27, 28]. What has been missing is direct, low-temperature evidence that the disappearance of competing order near optimal doping, and the associated change in ground-state symmetry, is accompanied by enhanced electronic interactions in the ground state.

A powerful technique for measuring low-temperature Fermi surface properties is the magnetic quantum-oscillation phenomenon, which directly accesses quasiparticle interactions through the effective mass [29]. Such measurements have been successful in identifying mass enhancements near QCPs in lower-T_c materials (e.g., $CeRhIn_5$ and $Ba(FeAs_xP_{1-x})_2$ [3, 5]), but the robustness of superconductivity near optimal doping in the cuprates has impeded access to the metallic ground-state. The Fermi surface in underdoped cuprates is known to be relatively small and electron-like [30, 31, 32, 33, 34] in contrast to overdoped cuprates where a much larger hole-like surface is observed [35]. This suggests the existence of broken translational symmetry in the underdoped cuprates that “reconstructs” the large hole-like surface into the smaller

electron-like surface, and this translational symmetry breaking is likely related to the charge order observed in the same doping range as the small Fermi pockets[27, 15]. Thus it is desirable to perform a systematic study of the doping dependence of these small pockets as optimal doping is approached within a single cuprate family. We use high magnetic fields, extending to over 90 T, to suppress superconductivity and access quantum oscillations of the underlying Fermi surface over nearly twice the range of dopings than previously possible in a single family (Fig. 1).

We report the observation of quantum oscillations in $YBa_2Cu_3O_{6+\delta}$ at $\delta = 0.75$, 0.80, and 0.86 (hole doping $p = 0.135, 0.140, \text{and } 0.152$), shown in Fig. 2A. Three regimes are clearly seen in the data: zero resistance in the vortex-solid state; finite resistance that increases strongly with field in the crossover to the normal state; and, magnetoresistance accompanied by quantum oscillations in the normal state. We subtract a smooth and monotonic background from the magnetoresistance to obtain the oscillatory component [36]. One can make two immediate observations: (1) at higher doping the oscillation amplitude grows faster with decreasing temperature; and (2), the oscillation frequency changes very little between $p = 0.135$ and $p = 0.152$. The first observation directly indicates an increasing effective mass; the second observation constrains the doping where the reconstruction from large to small Fermi surface takes place. We quantify these observations below.

The evolution of the cyclotron effective mass with doping, and how it relates to temperature dependence of the quantum oscillations, can be understood quantitatively within

the Lifshitz-Kosevich formalism, which has been used successfully to analyse oscillations in cuprates at lower hole doping [23, 32, 33, 34, 37]. The effective mass extracted from the quantum oscillation amplitude [36] is plotted as a function of doping in Fig. 3C, which reveals an increase in the mass by almost a factor of three from p = 0.116 to p = 0.152. Note that electron-phonon coupling is generally observed to decrease with increasing hole doping in the cuprates, ruling it out as the mechanism of mass enhancement [38], and suggesting instead that the mass enhancement comes from increased electron-electron interactions. The enhancement of the effective mass toward p ≈ 0.18 is consistent with the doping-dependent maxima observed in the upper critical field H_{c2} [39], and in the jump in the specific heat (Δγ) at T_c [40, 41], both of which are expected to be enhanced by the effective mass through the density of states (see Fig. 1). Maxima in thermodynamic quantities are typical of quantum-critical systems at their QCPs, having been observed in many heavy fermion systems [42] and an iron pnictide superconductor [5]. The fact that some physical quantities do not show an enhancement toward optimal doping in $YBa_2Cu_3O_{6+\delta}$, such as the superfluid density [43], may be related to the fact that different physical properties experience different renormalizations from interactions [44], or the fact that they are measured in the superconducting state where the gap may serve as a cut-off.

The quantum oscillation frequency F gives the Fermi surface area through the Onsager relation [29], $A_k = \frac{2\pi e}{\hbar} F$, where A_k is the Fermi surface area in momentum space perpendicular to the magnetic field. In contrast to the effective mass, which is enhanced by almost a factor of three, the Fermi surface area only evolves weakly toward optimal doping: Fig.

2B shows F increasing by roughly 20% from $p \approx 0.09$ to $p \approx 0.152$. The observation of the small Fermi surface pocket up to $p \approx 0.152$ requires that the reconstruction of the Fermi surface also persists up to this doping, strongly suggesting that the reconstruction is related to the incommensurate charge order also observed in this doping range [15, 25, 26, 27]. The large increase in effective mass with no accompanying large change in Fermi surface area is reminiscent of what is seen on approach to QCPs in $CeRh_2Si_2$, $CeRhIn_5$, and $BaFe_2(As_{1-x}P_x)_2$ [42, 5].

The connection between the mass enhancement we observe in quantum oscillations and high-T_c superconductivity is evident in Fig. 4, which shows successive T_c curves in increasing magnetic field. By 30 T—the third-highest curve in Figure 4—superconductivity persists only in two small domes centred around $p \approx 0.08$ and $p \approx 0.18$; by 50 T only the region around $p = 0.18$ remains. This phase diagram of $YBa_2Cu_3O_{6+\delta}$ in high field, with T_c first suppressed to zero around $p \approx 0.125$, closely resembles that of $La_{2-x}Ba_xCuO_4$ in zero field, where static charge and stripe order are observed [45]. To emphasize the enhancement of the effective mass, we plot $1/m^*$on this phase diagram (including previous m^* measurements at lower doping [46]). This shows a trend toward maximum mass enhancement at $p \approx 0.08$ and $p \approx 0.18$—the same dopings at which superconductivity is the most robust to applied magnetic fields. One possible scenario for $YBa_2Cu_3O_{6+\delta}$ is that critical fluctuations surrounding $p_{crit} \approx 0.08$ and $p_{crit} \approx 0.18$ provide two independent pairing mechanisms, analogous to the two superconducting domes in $CeCu_2Si_2$ that originate at antiferromagnetic and valence-transition QCP [47]. A second scenario is a single underlying pairing mechanism whose

strength varies smoothly with doping[7, 48], but where T_c enhanced at $p_{crit} \approx 0.08$ and $p_{crit} \approx 0.18$ by an increased density of states and/or by quantum-critical dynamics.

Our observed mass increase establishes the enhancement of electronic interactions approaching $p_{crit} \approx 0.18$. It is natural to ask whether this enhancement is caused by a quantum-critical point at $p_{crit} \approx 0.18$, and, subsequently, what is the associated broken-symmetry phase. The hole doping $p_{crit} \approx 0.18$ represents the juncture of several doping-dependent phenomena associated with underdoped cuprates. First, $p \approx 0.19$ represents the collapse to zero of energy scales associated with the formation of the pseudogap which onsets at temperature T^*[8]. Second, the onset of an anomalous polar Kerr rotation and neutron spin flip scattering both terminate at $p \approx 0.18$ [12, 13], representing an unidentified form of broken symmetry (that persists inside the superconducting phase for the Kerr experiment). Third, in high magnetic fields, the sign-change of the Hall coefficient in $YBa_2Cu_3O_{6+\delta}$ from positive to negative, and the anomaly in the Hall coefficient in $Bi_2Sr_{0.51}La_{0.49}CuO_{6+\delta}$, occur near p ≈ 0.18 [11, 49], suggesting that Fermi surface reconstruction from electron-like to hole-like occurs at this doping. Finally, $p \approx 0.18$ represents the maximum extent of incommensurate CDW order reported in several different experiments [26, 27, 15]. Although the Fermi surface reconstruction is likely related to this CDW order, its short correlation length and the weak doping dependence of its onset temperature appear to be at odds with the standard picture of long range order collapsing to $T = 0$ at a QCP [50]. Two scenarios immediately present themselves. In the first scenario, the suppression of superconductivity by an applied magnetic field allows the CDW to transition to long-range

order, as suggested by X-ray, NMR, and pulsed-echo ultrasound experiments [25, 26, 51]. In this first scenario, we would be observing a field-revealed QCP. In the second scenario, CDW order is co-existent with another form of order that also terminates near $p_{crit} \approx 0.18$. Such a coexistence is suggested by multiple experimental results, including but not limited to Nernst anisotropy[22], polarized neutron scattering [12] the anomalous polar Kerr effect[13]. In this second scenario, the CDW reconstructs the Fermi surface and the other hidden form of order drives quantum criticality. Regardless of the specific mechanism, and regardless of whether $p_{crit} = 0.18$ is a QCP in the traditional sense, the observation of an enhanced effective mass coincident with the region of most robust superconductivity establishes the importance of competing broken symmetry for high-T_c superconductivity.

References and Notes

[1] P Coleman, C Pepin, QM Si, and R Ramazashvili. How do fermi liquids get heavy and die? *Journal of Physics-Condensed Matter*, 130 (35):0 R723–R738, SEP 3 2001. ISSN 0953-8984. 10.1088/0953-8984/13/35/202.

[2] Louis Taillefer. Scattering and pairing in cuprate superconductors. In JS Langer, editor, *Annual Review of Condensed Matter Physics, Vol 1*, volume 1 of *Annual Review of Condensed Matter Physics*, pages 51–70. 2010. ISBN 978-0-8243-5001-7. 10.1146/annurev-conmatphys-070909-104117.

[3] H Shishido, R Settai, H Harima, and Y Onuki. A drastic change of the fermi surface at a critical pressure in CeRhIn $_5$: dHvA study under pressure. *Journal of the Physical Society of Japan*, 740 (4):0 1103–1106, Apr 2005. ISSN 0031-9015. 10.1143/JPSJ.74.1103.

[4] Philipp Gegenwart, Qimiao Si, and Frank Steglich. Quantum criticality in heavy-fermion metals. *Nature Physics*, 40 (3):0 186–197, Mar 2008. ISSN 1745-2473. 10.1038/nphys892.

[5] P. Walmsley, C. Putzke, L. Malone, I. Guillamon, D. Vignolles, C. Proust, S. Badoux, A. I. Coldea, M. D. Watson, S. Kasahara, Y. Mizukami, T. Shibauchi, Y. Matsuda, and A. Carrington. Quasiparticle Mass Enhancement Close to the Quantum Critical Point in BaFe $_2$(As $_{1-x}$P $_x$) $_2$. *Physical Review Letters*, 1100 (25), Jun 21 2013. ISSN 0031-9007. 10.1103/PhysRevLett.110.257002.

[6] P. Monthoux, D. Pines, and G. G. Lonzarich. Superconductivity without phonons. *Nature*, 4500 (7173):0 1177–1183, Dec 20 2007. ISSN 0028-0836. 10.1038/nature06480.

[7] PW Anderson, PA Lee, M Randeria, TM Rice, N Trivedi, and FC Zhang. The physics behind high-temperature superconducting cuprates: the 'plain vanilla' version of rvb. *Journal of Physics-Condensed Matter*, 160 (24):0 R755–R769, Jun 23 2004. ISSN 0953-8984. 10.1088/0953-8984/16/24/R02.

[8] JL Tallon and JW Loram. The doping dependence of T^* - what is the real $high - T_c$ phase diagram? *Physica C*, 3490 (1-2):0 53–68, Jan 1 2001. ISSN 0921-4534. 10.1016/S0921-4534(00)01524-0.

[9] G. S. Boebinger, Yoichi Ando, A. Passner, T. Kimura, M. Okuya, J. Shimoyama, K. Kishio, K. Tamasaku, N. Ichikawa, and S. Uchida. Insulator-to-metal crossover in the normal state of la2−x sr x cuo 4 near optimum doping. Phys. Rev. Lett., 77:5417–5420, Dec 1996. doi: 10.1103/PhysRevLett.77.5417.

[10] Yoichi Ando, Kouji Segawa, Seiki Komiya, and A. N. Lavrov. Electrical resistivity anisotropy from self-organized one dimensionality in high-temperature superconductors. Phys. Rev. Lett., 88:137005, Mar 2002. doi:10.1103/PhysRevLett.88.137005.

[11] Fedor F Balakirev, Jonathan B Betts, Albert Migliori, S Ono, Yoichi Ando, and Gregory S Boebinger. Signature of optimal doping in hall-effect measurements on a high-temperature superconductor. Nature, 424(6951):912–915, 2003.

[12] B. Fauqué, Y. Sidis, V. Hinkov, S. Pailhès, C. T. Lin, X. Chaud, and P. Bourges. Magnetic order in the pseudogap phase of high-T_C superconductors. *Phys. Rev. Lett.*, 96:0 197001, May 2006. 10.1103/PhysRevLett.96.197001. URL http://link.aps.org/doi/10.1103/PhysRevLett.96.197001.

[13] Jing Xia, Elizabeth Schemm, G. Deutscher, S. A. Kivelson, D. A. Bonn, W. N. Hardy, R. Liang, W. Siemons, G. Koster, M. M. Fejer, and A. Kapitulnik. Polar Kerr-effect

measurements of the high-temperature YBa $_2$Cu $_3$O $_{6+x}$ superconductor: Evidence for broken symmetry near the pseudogap temperature. *Physical Review Letters*, 1000 (12), Mar 28 2008. ISSN 0031-9007. 10.1103/PhysRevLett.100.127002.

[14] A. Shekhter, B. J. Ramshaw, R. D. McDonald, J. B. Betts, F. Balakirev, Ruixing Liang, W. N. Hardy, D. A. Bonn, Scott C. Riggs, and Albert Migliori. Bounding the pseudogap with a line of phase transitions in YBa $_2$Cu $_3$O $_{6+\delta}$. *Nature*, 4980 (7452):0 75–77, 2013.

[15] S Blanco-Canosa, A Frano, E Schierle, J Porras, T Loew, M Minola, M Bluschke, E Weschke, B Keimer, and M Le Tacon. Resonant x-ray scattering study of charge density wave correlations in yba _2 cu _3 o _{6 + x}. *Physical Review B,* 90:5 054513, Aug 2014. 10.1103/PhysRevB.90.054513.

[16] K Fujita, Chung Koo Kim, Inhee Lee, Jinho Lee, MH Hamidian, IA Firmo, S Mukhopadhyay, H Eisaki, S Uchida, MJ Lawler, E.-A. Kim, and J.C. Davis. Simultaneous transitions in cuprate momentum-space topology and electronic symmetry breaking. *Science,* 344 (6184) 612-616, May 2014. 10.1126/science.1248783.

[17] CM Varma. Pseudogap phase and the quantum-critical point in copper-oxide metals. *Physical Review Letters*, 830 (17):0 3538–3541, OCT 25 1999. ISSN 0031-9007. 10.1103/PhysRevLett.83.3538.

[18] S Chakravarty, RB Laughlin, DK Morr, and C Nayak. Hidden order in the cuprates. *Physical Review B*, 630 (9), MAR 1 2001. ISSN 0163-1829. 10.1103/PhysRevB.63.094503.

[19] Subir Sachdev. *Quantum phase transitions*. Wiley Online Library, 2007.

[20] Patrick A. Lee. From high temperature superconductivity to quantum spin liquid: progress in strong correlation physics. *Reports on Progress in Physics*, 710 (1), Jan 2008. ISSN 0034-4885. 10.1088/0034-4885/71/1/012501.

[21] SA Kivelson, E Fradkin, and VJ Emery. Electronic liquid-crystal phases of a doped Mott insulator. *Nature*, 3930 (6685):0 550–553, Jun 11 1998. ISSN 0028-0836.

[22] R. Daou, J. Chang, David LeBoeuf, Olivier Cyr-Choinière, Francis Laliberte, Nicolas Doiron-Leyraud, B. J. Ramshaw, Ruixing Liang, D. A. Bonn, W. N. Hardy, and Louis Taillefer.

Broken rotational symmetry in the pseudogap phase of a high-T_c superconductor. *Nature*, 4630 (7280):0 519–522, Jan 28 2010. ISSN 0028-0836. 10.1038/nature08716.

[23] B. J. Ramshaw, Baptiste Vignolle, James Day, Ruixing Liang, W. N. Hardy, Cyril Proust, and D. A. Bonn. Angle dependence of quantum oscillations in $YBa_2Cu_3O_{6.59}$ shows free-spin behaviour of quasiparticles. *Nature Physics*, 70 (3):0 234–238, Mar 2011. ISSN 1745-2473. 10.1038/NPHYS1873. URL http://dx.doi.org/10.1038/nphys1873.

[24] G. Ghiringhelli, M. Le Tacon, M. Minola, S. Blanco-Canosa, C. Mazzoli, N. B. Brookes, G. M. De Luca, A. Frano, D. G. Hawthorn, F. He, T. Loew, M. Moretti Sala, D. C. Peets, M. Salluzzo, E. Schierle, R. Sutarto, G. A. Sawatzky, E. Weschke, B. Keimer, and L. Braicovich. Long-range incommensurate charge fluctuations in (y,nd)ba2cu3o6+x. *SCIENCE*, 3370 (6096):0 821–825, AUG 17 2012. ISSN 0036-8075. 10.1126/science.1223532.

[25] J. Chang, A. T. Blackburn, N. B. Holmes, J. Christensen, J. Larsen, J. Mesot, Ruixing Liang, D. A. Bonn, W. N. Hardy, A. Watenphul, M. v. Zimmerman, E. M. Forgan, and S. M. Hayden. Direct observation of competition between superconductivity and charge density wave order in $YBa_2Cu_3O_y$. *Nature Physics*, Oct 2012. 10.1038/nphys2456. URL http://dx.doi.org/10.1038/nphys2456.

[26] Tao Wu, Hadrien Mayaffre, Steffen Krämer, Mladen Horvatic′, Claude Berthier, Philip L Kuhns, Arneil P Reyes, Ruixing Liang, WN Hardy, DA Bonn, et al. Emergence of charge order from the vortex state of a high-temperature superconductor. *Nature communications*, 4, 2013.

[27] M Huecker, NB Christensen, AT Holmes, E Blackburn, EM Forgan, Ruixing Liang, DA Bonn, WN Hardy, O Gutowski, M v Zimmermann, et al. Competing charge, spin, and superconducting orders in underdoped yba2cu3oy. *Physical Review B*, 90:5 054514. Aug 2014. 10.1103/PhysRevB.90.054514

[28] R. Comin, A. Frano, M. M. Yee, Y. Yoshida, H. Eisaki, E. Schierle, E. Weschke, R. Sutarto, F. He, A. Soumyanarayanan, Yang He, M. Le Tacon, I. S. Elfimov, Jennifer E. Hoffman, G. A. Sawatzky, B. Keimer, and A. Damascelli. Charge order driven by fermi-arc instability in bi2sr2-xlaxcuo6+delta. *Science*, 3430 (6169):0 390–392, JAN 24 2014. ISSN 0036-8075. 10.1126/science.1242996.

[29] D. Shoenberg. *Magnetic oscillations in metals*. Cambridge monographs on

physics. Cambridge University Press, 1984. ISBN 9780521224802.

[30] Nicolas Doiron-Leyraud, Cyril Proust, David LeBoeuf, Julien Levallois, Jean-Baptiste Bonnemaison, Ruixing Liang, D. A. Bonn, W. N. Hardy, and Louis Taillefer. Quantum Oscillations and the Fermi Surface in an Underdoped High-T $_c$ Superconductor. *Nature*, 4470 (7144):0 565–568, May 31 2007. ISSN 0028-0836. 10.1038/nature05872.

[31] David LeBoeuf, Nicolas Doiron-Leyraud, Julien Levallois, R. Daou, J.-B. Bonnemaison, N. E. Hussey, L. Balicas, B. J. Ramshaw, Ruixing Liang, D. A. Bonn, W. N. Hardy, S. Adachi, Cyril Proust, and Louis Taillefer. Electron pockets in the fermi surface of hole-doped high-t-c superconductors. *Nature*, 4500 (7169):0 533–536, Nov 22 2007. ISSN 0028-0836. 10.1038/nature06332.

[32] E. A. Yelland, J. Singleton, C. H. Mielke, N. Harrison, F. F. Balakirev, B. Dabrowski, and J. R. Cooper. Quantum oscillations in the underdoped cuprate $\mathrm{yba_2cu_4o_8}$. *Phys. Rev. Lett.*, 100:0 047003, Feb 2008. 10.1103/PhysRevLett.100.047003. URL http://link.aps.org/doi/10.1103/PhysRevLett.100.047003.

[33] A. F. Bangura, J. D. Fletcher, A. Carrington, J. Levallois, M. Nardone, B. Vignolle, P. J. Heard, N. Doiron-Leyraud, D. LeBoeuf, L. Taillefer, S. Adachi, C. Proust, and N. E. Hussey. Small fermi surface pockets in underdoped high temperature superconductors: Observation of shubnikov-de haas oscillations in yba(2)cu(4)o(8). *Physical Review Letters*, 1000 (4), FEB 1 2008. ISSN 0031-9007. 10.1103/PhysRevLett.100.047004.

[34] Neven Barišic′, Sven Badoux, Mun K Chan, Chelsey Dorow, Wojciech Tabis, Baptiste Vignolle, Guichuan Yu, Jérôme Béard, Xudong Zhao, Cyril Proust, and Martin Greven. Universal quantum oscillations in the underdoped cuprate superconductors. *Nature Physics*, 90 (12):0 761–764, 2013.

[35] B Vignolle, A Carrington, RA Cooper, MMJ French, AP Mackenzie, C Jaudet, D Vignolles, Cyril Proust, and NE Hussey. Quantum oscillations in an overdoped high-tc superconductor. Nature, 455(7215):952–955, 2008.

[36] Materials and Methods, Supplementary Text, and Supplementary Figures are available as supporting material on Science Online.

[37] Suchitra E. Sebastian, N. Harrison, M. M. Altarawneh, Ruixing Liang, D. A. Bonn, W. N. Hardy, and G. G. Lonzarich. Fermi-liquid behavior in an underdoped high-T_{c}

superconductor. *Phys. Rev. B*, 81:0 140505, Apr 2010a. 10.1103/PhysRevB.81.140505. URL http://link.aps.org/doi/10.1103/PhysRevB.81.140505.

[38] Z-X Shen, A Lanzara, S Ishihara, and N Nagaosa. Role of the electron-phonon interaction in the strongly correlated cuprate superconductors. *Philosophical Magazine B*, 820 (13):0 1349–1368, 2002.

[39] G Grissonnanche, O Cyr-Choiniere, F Laliberte, S Rene de Cotret, A Juneau-Fecteau, S Dufour-Beausejour, M-E Delage, D LeBoeuf, J Chang, B.J. Ramshaw, D. A. Bonn, W. N. Hardy, Ruixing Liang, S. Adachi, N. E. Hussey, B. Vignolle, C. Proust, M. Sutherland, S. Kramer, J.-H. Park, D. Graf, N. Doiron-Leyraud, and Louis. Taillefer. Direct measurement of the upper critical field in a cuprate superconductor. *Nature Communications*, 5, Feb 2014. /10.1038/ncomms4280.

[40] J. W. Loram, K. A. Mirza, J. R. Cooper, and W. Y. Liang. Electronic specific heat of $\mathrm{yba_2cu_3o_{6+x}}$ from 1.8 to 300 k. *Phys. Rev. Lett.*, 71:0 1740–1743, Sep 1993. 10.1103/PhysRevLett.71.1740. URL http://link.aps.org/doi/10.1103/PhysRevLett.71.1740.

[41] JW Loram, KA Mirza, JR Cooper, and JL Talloon. Specific heat evidence on the normal state pseudogap. *Journal of Physics and Chemistry of Solids*, 590 (10-12):0 2091–2094, Oct-Dec 1998. ISSN 0022-3697. 10.1016/S0022-3697(98)00180-2. International Conference on Spectroscopies in Novel Superconductors (SNS'97), CAPE COD, MA, SEP 14-18, 1997.

[42] Rikio Settai, Tetsuya Takeuchi, and Yoshichika $\overline{\mathrm{O}}$nuki. Recent advances in ce-based heavy-fermion superconductivity and fermi surface properties. *Journal of the Physical Society of Japan*, 760 (5), 2007.

[43] J. E. Sonier, S. A. Sabok-Sayr, F. D. Callaghan, C. V. Kaiser, V. Pacradouni, J. H. Brewer, S. L. Stubbs, W. N. Hardy, D. A. Bonn, R. Liang, and W. A. Atkinson. Hole-doping dependence of the magnetic penetration depth and vortex core size in Yba 2 cu 3 o y : Evidence for stripe correlations near 1/8 hole doping. Phys. Rev. B, 76:134518, Oct 2007. doi:10.1103/PhysRevB.76.134518.

[44] AJ Leggett. Inequalities instabilites and renormalization in metals and other fermi liquids.Annals of Physics, 46(1):76–&, 1968. ISSN 0003-4916. doi:10.1016/0003-4916(68)90304-7.

[45] M. Huecker, M. v. Zimmermann, G. D. Gu, Z. J. Xu, J. S. Wen, Guangyong Xu, H. J. Kang, A. Zheludev, and J. M. Tranquada. Stripe order in superconducting La $_{2-x}$Ba $_x$CuO $_4$ (0.095 <= x <= 0.155). *Physical Review B*, 830 (10), Mar 17 2011. ISSN 1098-0121.

10.1103/PhysRevB.83.104506.

[46] Suchitra E. Sebastian, N. Harrison, M. M. Altarawneh, C. H. Mielke, Ruixing Liang, D. A. Bonn, W. N. Hardy, and G. G. Lonzarich. Metal-insulator quantum critical point beneath the high T $_c$ superconducting dome. *Proceedings of the National Academy of Sciences of the United States of America*, 1070 (14):0 6175–6179, Apr 6 2010b. ISSN 0027-8424.

[47] HQ Yuan, FM Grosche, M Deppe, C Geibel, G Sparn, and F Steglich. Observation of two distinct superconducting phases in CeCu $_2$Si $_2$. *Science*, 3020 (5653):0 2104–2107, Dec 19 2003. ISSN 0036-8075. 10.1126/science.1091648.

[48] M. Le Tacon, G. Ghiringhelli, J. Chaloupka, M. Moretti Sala, V. Hinkov, M. W. Haverkort, M. Minola, M. Bakr, K. J. Zhou, S. Blanco-Canosa, C. Monney, Y. T. Song, G. L. Sun, C. T. Lin, G. M. De Luca, M. Salluzzo, G. Khaliullin, T. Schmitt, L. Braicovich, and B. Keimer. Intense paramagnon excitations in a large family of high-temperature superconductors. *Nature PhysicS*, 70 (9):0 725–730, SEP 2011. ISSN 1745-2473. 10.1038/NPHYS2041.

[49] David LeBoeuf, Nicolas Doiron-Leyraud, B. Vignolle, Mike Sutherland, B. J. Ramshaw, J. Levallois, R. Daou, Francis Laliberté, Olivier Cyr-Choinière, Johan Chang, Y. J. Jo, L. Balicas, Ruixing Liang, D. A. Bonn, W. N. Hardy, Cyril Proust, and Louis Taillefer. Lifshitz critical point in the cuprate superconductor $\mathrm{yba_2cu_3o}_y$ from high-field hall effect measurements. *Phys. Rev. B*, 83:0 054506, Feb 2011. 10.1103/PhysRevB.83.054506. URL http://link.aps.org/doi/10.1103/PhysRevB.83.054506.

[50] Laimei Nie, Gilles Tarjus, and Steven Allan Kivelson. Quenched disorder and vestigial nematicity in the pseudogap regime of the cuprates. *Proceedings of the National Academy of Sciences of the United States of America*, 1110 (22):0 7980–7985, JUN 3 2014. ISSN 0027-8424. 10.1073/pnas.1406019111.

[51] David LeBoeuf, S. Kraemer, W. N. Hardy, Ruixing Liang, D. A. Bonn, and Cyril Proust. Thermodynamic phase diagram of static charge order in underdoped yba2cu3oy. *Nature Physics*, 90 (2):0 79–83, Feb 2013. ISSN 1745-2473.

[52] Baptiste Vignolle, David Vignolles, David LeBoeuf, Stephane Lepault, Brad Ramshaw, Ruixing Liang, D. A. Bonn, W. N. Hardy, Nicolas Doiron-Leyraud, A. Carrington, N. E. Hussey, Louis Taillefer, and Cyril Proust. Quantum oscillations and the Fermi surface of high-temperature cuprate superconductors. Comptes Rendus Physique, 12(5-6):446–460, Jun-Aug

2011. ISSN 1631-0705. doi:10.1016/j.crhy.2011.04.011.

[53] John Singleton, Clarina de la Cruz, R. D. McDonald, Shiliang Li, Moaz Altarawneh, Paul Goddard, Isabel Franke, Dwight Rickel, C. H. Mielke, Xin Yao, and Pengcheng Dai. Magnetic Quantum Oscillations in $YBa_2Cu_3O_{6.61}$ and $YBa_2Cu_3O_{6.69}$ in Fields of Up to 85 T: Patching the Hole in the Roof of the Superconducting Dome. *Phys. Rev. Lett.*, 104:0 086403, Feb 2010. 10.1103/PhysRevLett.104.086403. URL http://link.aps.org/doi/10.1103/PhysRevLett.104.086403.

[54] F. Coneri, S. Sanna, K. Zheng, J. Lord, and R. De Renzi. Magnetic states of lightly hole-doped cuprates in the clean limit as seen via zero-field muon spin spectroscopy. *Phys. Rev. B*, 81:0 104507, Mar 2010. 10.1103/PhysRevB.81.104507. URL http://link.aps.org/doi/10.1103/PhysRevB.81.104507.

[55] Y Ando, S Komiya, K Segawa, S Ono, and Y Kurita. Electronic phase diagram of high-T_c cuprate superconductors from a mapping of the in-plane resistivity curvature. *Physical Review Letters*, 930 (26), Dec 31 2004. ISSN 0031-9007. 10.1103/PhysRevLett.93.267001.

[56] Suchitra E. Sebastian, Neil Harrison, and Gilbert G. Lonzarich. Towards resolution of the Fermi surface in underdoped high-T_c superconductors. *Reports on Progress in Physics*, 750 (10), Oct 2012. ISSN 0034-4885. 10.1088/0034-4885/75/10/102501.

[57] B. J. Ramshaw, James Day, Baptiste Vignolle, David LeBoeuf, P. Dosanjh, Cyril Proust, Louis Taillefer, Ruixing Liang, W. N. Hardy, and D. A. Bonn. Vortex lattice melting and H_{c2} in underdoped $YBa_2Cu_3O_y$. *Phys. Rev. B*, 86:0 174501, Nov 2012. 10.1103/PhysRevB.86.174501. URL http://link.aps.org/doi/10.1103/PhysRevB.86.174501.

[58] M Von Zimmermann, JR Schneider, T Frello, NH Andersen, J Madsen, M Kall, HF Poulsen, R Liang, P Dosanjh, and WN Hardy. Oxygen-ordering superstructures in underdoped $YBa_2Cu_3O_{6+x}$ studied by hard x-ray diffraction. *Physical Review B*, 680 (10):0 104515, Sep 1 2003. ISSN 1098-0121. 10.1103/PhysRevB.68.104515. URL http://link.aps.org/doi/10.1103/PhysRevB.85.104515.

Acknowledgements

This work was performed at the National High Magnetic Field Laboratory, and was supported by the US Department of Energy BES “Science at 100 T," the National Science

Foundation DMR-1157490, the State of Florida, the Natural Science and Engineering Research Council of Canada and the Canadian Institute for Advanced Research. S.E.S. acknowledges support from the Royal Society and the European Research Council under the European Union's Seventh Framework Programme (FP7/2007-2013) / ERC Grant Agreement no. 337425. The authors gratefully acknowledge discussions with S. Chakravarty, S. Kivelson, M. Le Tacon, K.A. Modic, C. Proust, A. Shekhter, and L. Taillefer. We are indebted to J. Baglo for sharing his results on the effect of quenched oxygen disorder on the microwave scattering rate in $YBa_2Cu_3O_{6+\delta}$: without this advance, oscillations would not have been observed. Finally, we would like to acknowledge the entire 100 T operations team at the pulsed field facility for their support during the experiment. Full resistivity curve are available in the Supporting Online Material.

B.J.R., S.E.S., R.D.M., B.T., Z.Z., J.B.B., and N.H. performed the high-field resistivity measurements at the National High Magnetic Field Laboratory-Pulsed Field Facility. B.J.R., J.D., R.L., D.A.B., and W.N.H. grew and prepared the samples at the University of British Columbia. B.J.R. analysed the data and wrote the manuscript, with contributions from S.E.S., R.D.M., N.H., J.D, D.A.B., and W.N.H.

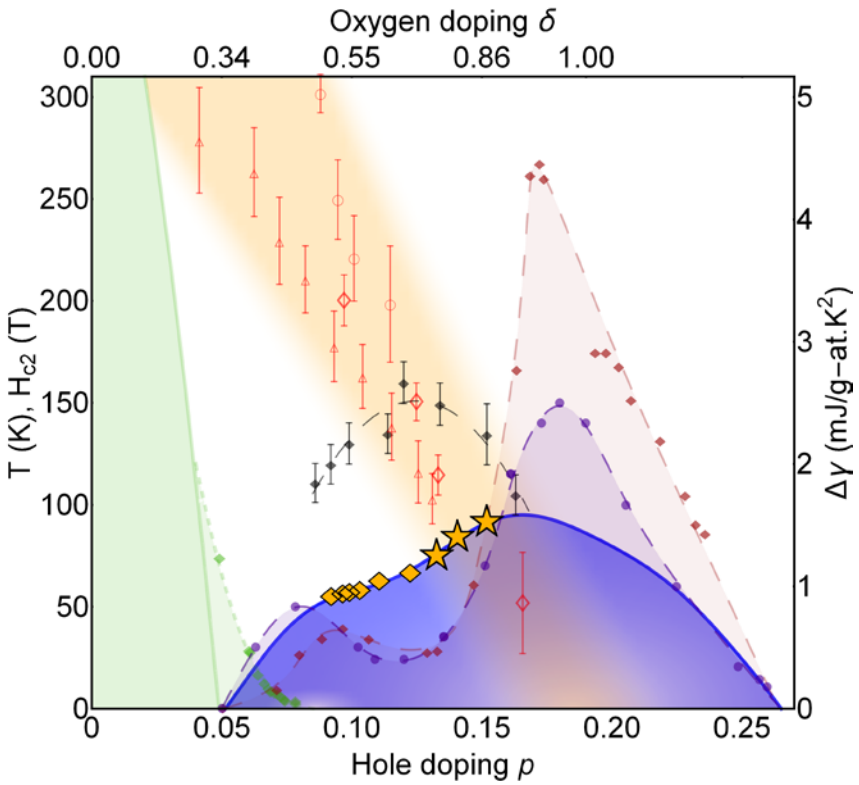


Fig. 1: Cuprate temperature-doping phase diagram. Long-range antiferromagnetic order (solid green line) gives way to superconductivity (solid blue line) near $p = 0.05$. Orange diamonds designate dopings where quantum oscillations have been observed previously[52, 53], and stars denote the new dopings presented in this paper. Short-range antiferromagnetic order (green diamonds) terminates at a quantum critical point at $p = 0.08$ [46, 54]; beyond $p = 0.08$, short-range charge order onsets above T_c (solid black diamonds [15, 27]). The charge order, the onset of the pseudogap (as defined by neutron spin-flip scattering (open red circles)[12], the polar Kerr effect (open red diamonds[13]), and the change in the slope of resistivity with temperature (open red triangles[55])) terminate near $p = 0.18$, suggesting the possibility of a quantum critical point at this doping. Two thermodynamic quantities show enhancement near the critical dopings: the jump in the specific heat at T_c($\Delta\gamma$, maroon diamonds [40, 41]), and the upper critical field (H_{c2}, purple points [39]).

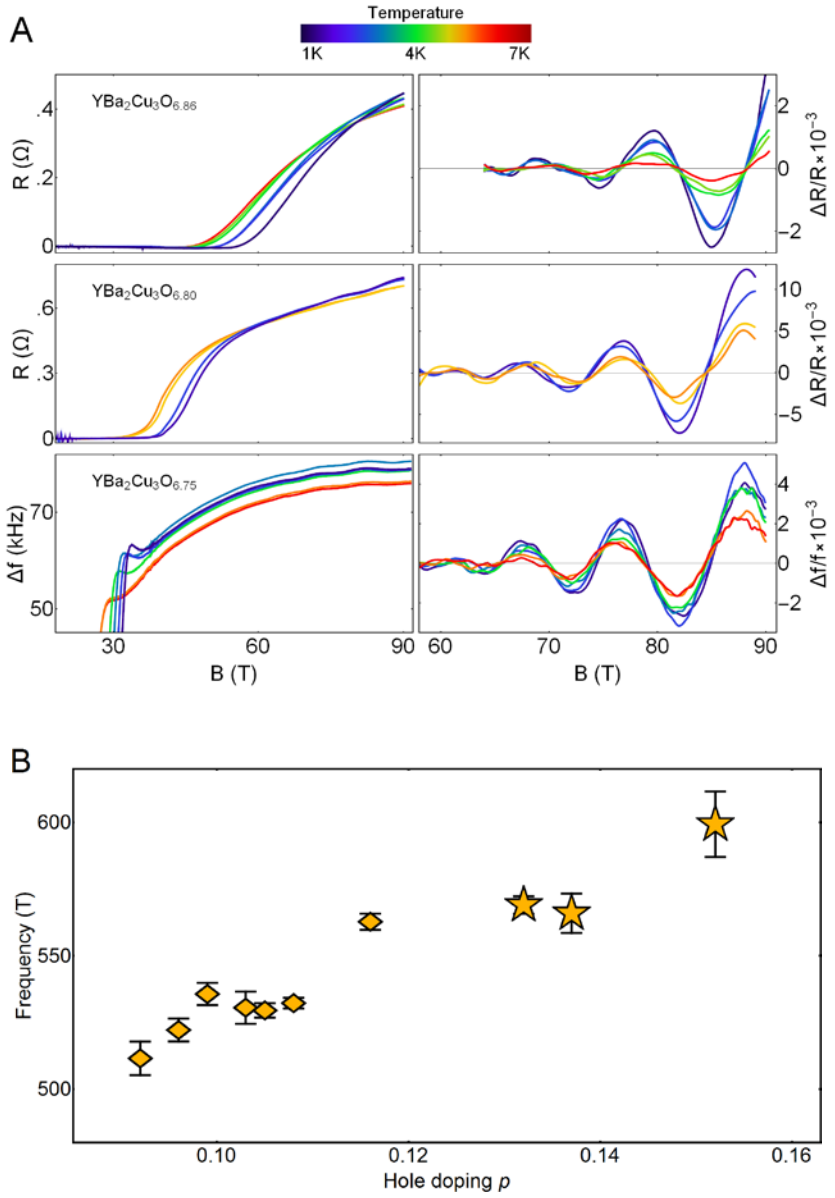


Fig. 2: Quantum oscillations of the magnetoresistance in $YBa_2Cu_3O_{6+\delta}$**.** (A) The bare (left panels) and oscillatory component (right panels) of the magnetoresistance. $\hat{c}$-axis transport was measured for $\delta = 0.80$ and 86; skin depth, measured via frequency shift of an oscillatory circuit [36], was measured for $\delta = 0.75$. A smooth, non-oscillatory background is removed from the data to extract the oscillatory component [36]. The quantum oscillation amplitude is suppressed by a factor of two between 1.5 and 6 K in $YBa_2Cu_3O_{6.75}$, compared to a factor of five

over the same temperature range in $YBa_2Cu_3O_{6.86}$, indicating an increased effective mass for the higher doped sample. **(B)** Quantum oscillation frequency, proportional to Fermi-surface area, as a function of hole doping, with dopings below $p = 0.12$ taken from [56]. The frequencies and their uncertainties were obtained as described in the Materials and Methods [36].

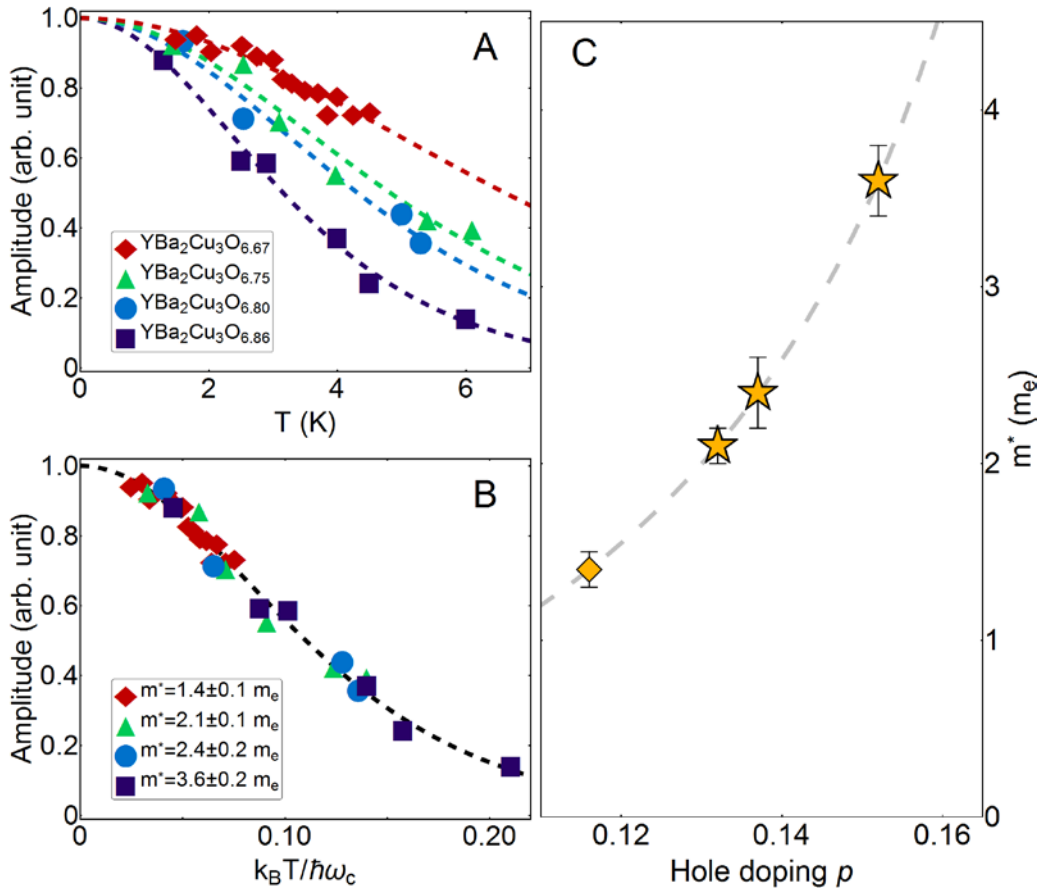


Fig. 3: The quasiparticle effective mass in $YBa_2Cu_3O_{6+\delta}$**.** Quantum oscillation amplitude **(A)** as a function of temperature, and **(B)** as a function of the ratio of thermal to cyclotron energy $k_BT/\hbar\omega_c$. Also included is detailed temperature dependence of $YBa_2Cu_3O_{6.67}$—a composition at which oscillations have previously been reported [53]. (A) illustrates the increase in m^* with

increased hole doping, with fits to Eq. 1. (B) shows the same data versus $k_B T/\hbar\omega_c^*$, where $\omega_c^* = eB/m^*$: this scaling with m^* shows the robustness of the fit across the entire doping and temperature range. **(C)** The effective mass as a function of hole doping; error bars are the standard error from regression of Eq. 1 to the data. The dashed line is a guide to the eye.

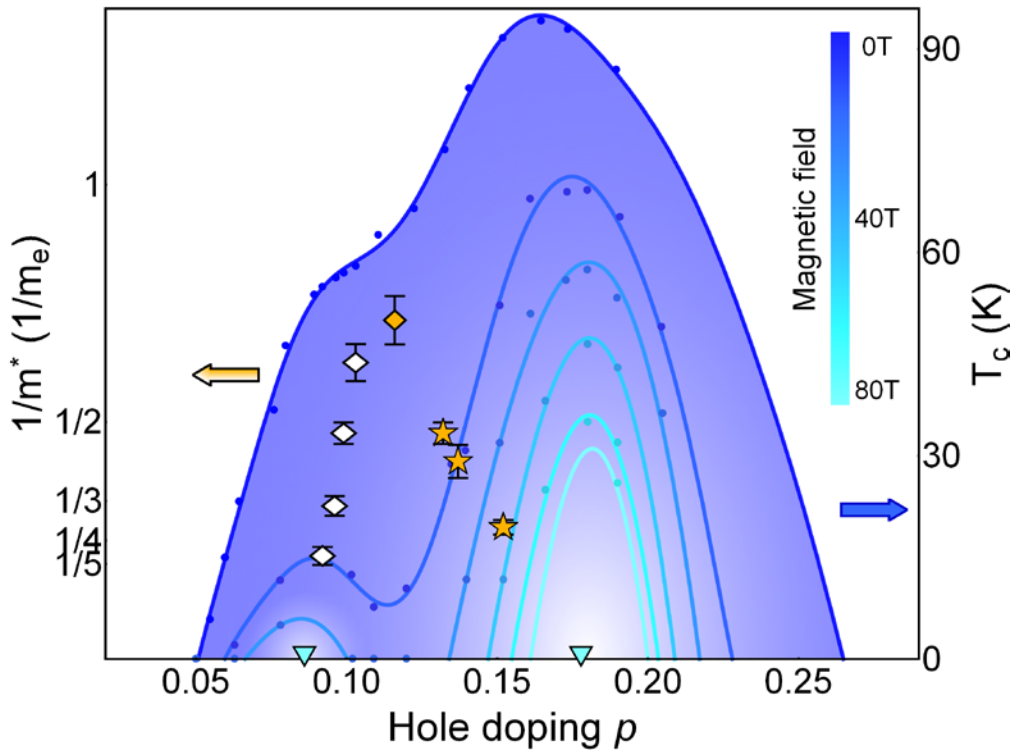


Fig. 4: A quantum critical point near optimal doping. The blue curves correspond to T_c, as defined by the resistive transition (right axis), at magnetic fields of 0, 15, 30, 50, 70, and 82 T (some data points taken from [39], [57].) As the magnetic field is increased, the superconducting T_c is suppressed. By 30 T two separate domes remain, centred around $p \approx 0.08$ and $p \approx 0.18$; by 82 T only the dome at $p \approx 0.18$ remains. The inverse of the

effective mass has been overlaid on this phase diagram (left axis), extrapolating to maximum mass enhancement at at $p \approx 0.08$ and $p \approx 0.18$ (white points taken from [56]). This makes explicit the connection between effective mass enhancement and the robustness of superconductivity.

Supplementary Materials

Materials and Methods
Supplementary Text
Figs. S1 to S15
References [59-69]

Supplementary Information: Quasiparticle mass enhancement approaching optimal doping in a high-T_c superconductor

B. J. Ramshaw, S. E. Sebastian, R. D. McDonald, James Day, B. Tan, Z. Zhu, J.B. Betts, Ruixing Liang, D. A. Bonn, W. N. Hardy, N. Harrison

March 2, 2022

Materials and Methods

SAMPLES:

$YBa_2Cu_3O_{6+\delta}$ samples were prepared for transport measurements in the same manner as in our previous studies.[30, 23] Prior to measurement, samples were heated above the ortho-III and ortho-VIII phase transition temperatures[58] to disorder the oxygen in the chains, and then quenched in liquid nitrogen. This process changes the nature of the oxygen defects in $YBa_2Cu_3O_{6+\delta}$ while preserving the total oxygen content, and enabled the observation of quantum oscillations by increasing the quasiparticle lifetime.

MEASUREMENT:

Four-point $\hat{c}$-axis electrical resistance was measured for $YBa_2Cu_3O_{6.80}$ and $YBa_2Cu_3O_{6.86}$ using a digital lock-in amplifier. Skin-depth, proportional to $\hat{a}-\hat{b}$–plane resistance, was measured using a proximity detector oscillator on $YBa_2Cu_3O_{6.67}$ and $YBa_2Cu_3O_{6.75}$.[46] All pulsed field measurements—up to 92 T for $YBa_2Cu_3O_{6.86}$, $YBa_2Cu_3O_{6.80}$, and $YBa_2Cu_3O_{6.75}$; up to 65 T for $YBa_2Cu_3O_{6.67}$—were made at the National High Magnetic Field Laboratory–Pulsed Field Facility.

ANALYSIS:

The temperature-dependent amplitude $A(T)$ is extracted from the oscillatory magnetoresistance by fitting the standard Lifshitz-Kosevich expression for a quasi-2D Fermi surface[23] $\frac{\Delta R}{R} = A(T)\, e^{-\frac{\pi}{\omega_c \tau}} \cos\left(\frac{2\pi F}{B}\right) J_0\left(\frac{2\pi \Delta F}{B}\right)$ at each temperature, keeping τ, F, and ΔF fixed for a particular doping. The mass is then obtained by fitting the amplitude to $A(T) = \frac{2\pi^2 \frac{k_B T}{\hbar \omega_c^\star}}{\sinh\left(2\pi^2 \frac{k_B T}{\hbar \omega_c^\star}\right)}$.

Because of the small number of oscillations available at high doping, the frequency F was obtained in three different ways to check for consistency: by fitting the oscillatory component to the Lifshitz-Kosevich expression above; by Fourier-transforming the oscillatory data; and by Landau-indexing the oscillation peak positions [52]. The uncertainties in F shown in Fig. 2B were obtained from the Fourier transform peak widths. While there are systematic differences of about 3% between the three methods of frequency determination, the trend of F with hole doping p is the same to within the uncertainty.

Supplementary Text

The Fermi surface of a layered material, such as a cuprate high-T_c superconductor, is generally composed of cylinders that extend along the inter-layer direction, with finite interlayer tunnelling warping the cylinders [59]. Quantum oscillations, which are sensitive to extremal Fermi surface areas perpendicular to an applied magnetic field, are used to map out this geometry in detail. The total magnetoresistance $R(B)$ of $YBa_2Cu_3O_{6+\delta}$, with both field and current applied parallel to the $\hat{c}$-axis, is composed of a background magnetoresistance, $R_0(B)$, with an oscillatory component $A_{osc}(B)$ that is scaled by the size of the background resistance[29]:

$$R(B) = R_0(B)\left(1 + A_{osc}(B)\right). \tag{S1}$$

The oscillatory component $A_{osc}(B)$ for a simple quasi-2D Fermi surface is described within the Lifshitz-Kosevich formalism as (see [23]):

$$A_{osc}(B) = AR_T R_D \cos\left(\frac{2\pi F}{B}\right) J_0\left(\frac{2\pi \Delta F}{B}\right) \tag{S2}$$

$$R_D = e^{-\frac{\pi}{\omega_c \tau}} \tag{S3}$$

$$R_T = \frac{2\pi^2 \frac{k_B T}{\hbar \omega_c}}{\sinh\left(2\pi^2 \frac{k_B T}{\hbar \omega_c}\right)}, \tag{S4}$$

where A is an amplitude factor, F is the oscillation frequency (proportional to the area of the Fermi surface perpendicular to the applied field), ΔF is the first harmonic of warping in the k_z direction, $\omega_c \equiv eB/m^\star$ is the cyclotron frequency, $m^\star$ is the cyclotron effective mass, and τ is the quasiparticle lifetime. Since we are only interested in the *temperature* dependence of the oscillation amplitude, the exact Fermi surface geometry (which constrains the *field* dependence) is relatively unimportant here [60, 23, 61]. Since the masses for different frequency components have been reported to be very similar [56], the use of Equation S2 is preferable as a minimal model that prevents "over-parametrization" of the data set.

The desired component in Equation S1 is the oscillatory component, $A_{osc}(B)$, and thus the background magnetoresistance $R_0(B)$ must be removed from the data. This is done by fitting Equation S1 to the measured data at each temperature, together with a polynomial (generally 3rd or 4th order) for the background:

$$R(B) = \left(a_0 + a_1 B + a_2 B^2 + a_3 B^3 ...\right)\left(1 + A_{osc}(B)\right), \tag{S5}$$

where the coefficients a_i are free parameters, and $A_{osc}(B)$ contains the Fermi surface parameters A, F, ΔF, $m^\star$, and τ (see Equation S1). The oscillatory component $A_{osc}(B)$ is then obtained by dividing out the background polynomial and subtracting 1 from the data. Because the fit parameters A, F, ΔF, $m^\star$, and τ are generally temperature-independent [29], only the polynomial coefficients a_i vary as the background magnetoresistance changes with temperature.

Data and fits

The following four sections present all of the fits to the data for the dopings discussed in the main text, including new data taken for $YBa_2Cu_3O_{6.67}$ to precisely determine the mass (not shown in Figure 2a of the main text because of the lower field range). For each doping, the vertical span for the plots at each temperature is the same: this allows the evolution of the oscillation amplitude to be tracked by eye without background subtraction. For $YBa_2Cu_3O_{6.80}$ and $YBa_2Cu_3O_{6.86}$, where the oscillation amplitude becomes small due to the increase in effective mass, we also present the derivatives of the data.

$YBa_2Cu_3O_{6.67}$

Quantum oscillations were measured in $YBa_2Cu_3O_{6.67}$ using the proximity detector oscillator (PDO) technique. This is a contactless resistivity probe, where the sample is placed next to a pickup coil that is part of an oscillatory circuit. Changes in sample resistance as a function of magnetic field change the sample skin depth, tuning the inductance of the coil and producing a frequency shift in the oscillator self-resonance.

Figure S1 shows the raw frequency-shift data for $YBa_2Cu_3O_{6.67}$ at six of the fourteen measured temperatures (spanning the full temperature range), along with the polynomial background in black and the full fit to Equation S5 in red. The fits yield $F = 563 \pm 3$ T, $\Delta F = 15 \pm 6$ T, $\tau = 0.08 \pm 0.01$ ps, and $m^\star = 1.4 \pm 0.1$ m_e. Of the four dopings presented here, only $YBa_2Cu_3O_{6.67}$ has a significant contribution from a third frequency of $F = 519 \pm 5$ T. The background-free data from these fits at all temperatures, along with the mass fit from the oscillation amplitude, is shown in Figure S2.

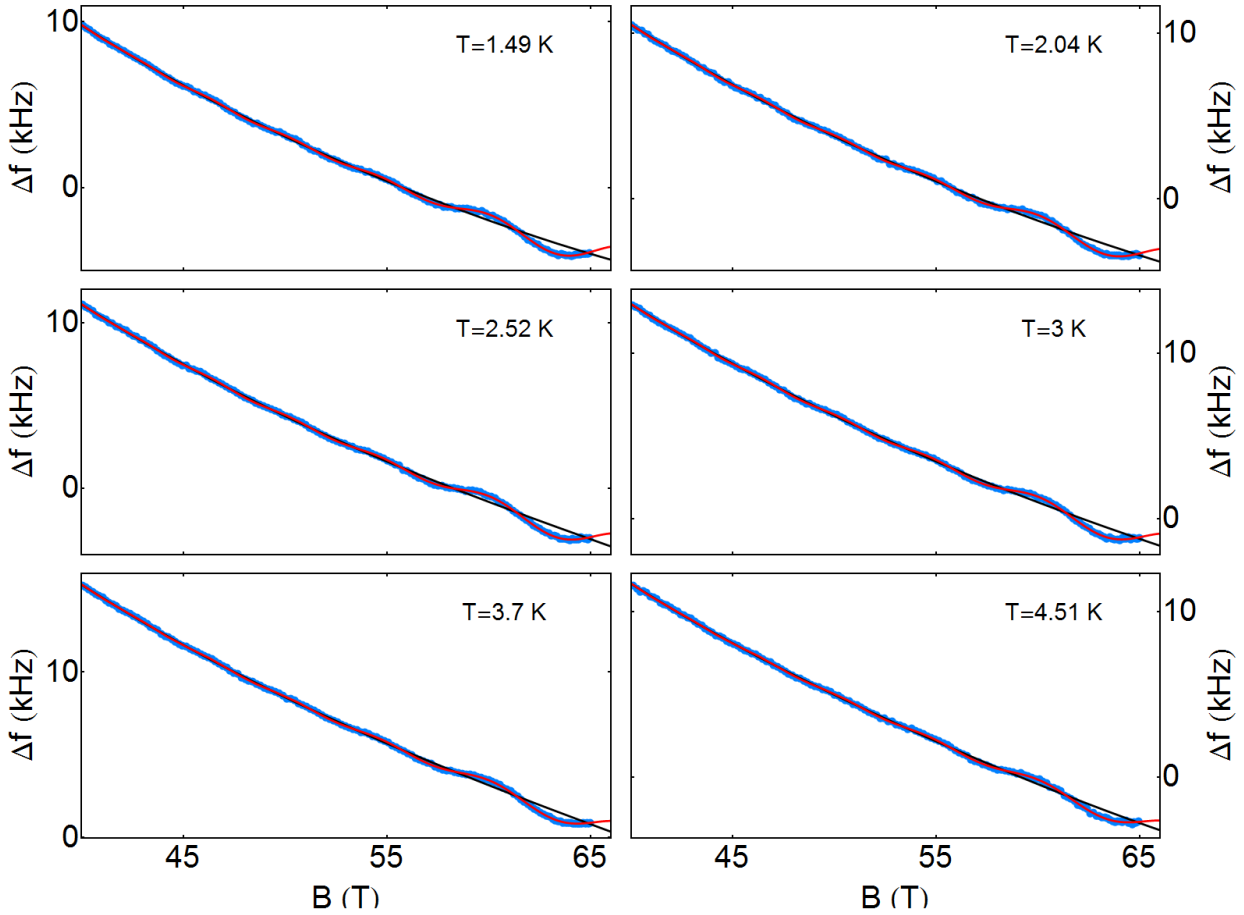


Fig. S1: Shift in the proximity-diode oscillator frequency for $YBa_2Cu_3O_{6.67}$, proportional to the skin depth (and therefore resistivity) at ~ 30 MHz: the raw data is in blue; the fit to Equation S2 plus a background is in red; the background alone is in black. The data at six temperatures, spanning the entire temperature range, are shown here. All panels have the same vertical span.

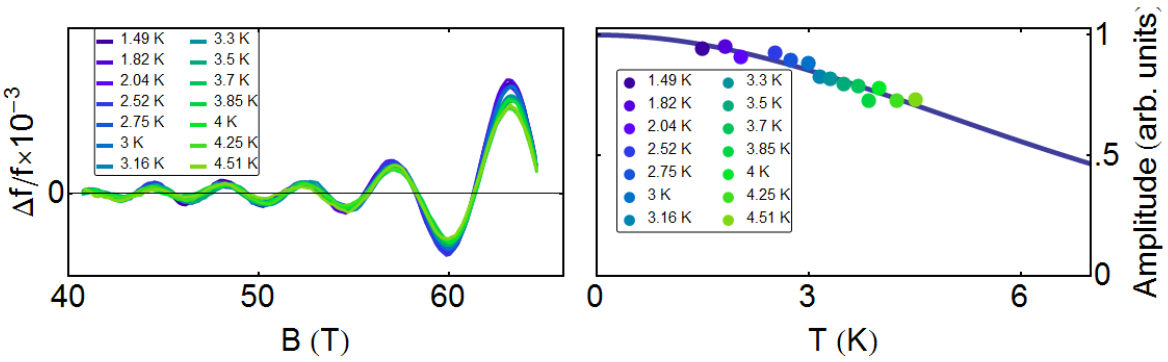


Fig. S2: *Left panel:* Relative frequency shift with respect to the background, proportional to $\Delta\rho/\rho$, for $YBa_2Cu_3O_{6.67}$ at each temperature with a background subtracted. *Right panel:* Fit to the oscillation amplitude, yielding $m^\star = 1.4 \pm 0.1$.

$YBa_2Cu_3O_{6.75}$

The same contactless magnetotransport technique that was performed on $YBa_2Cu_3O_{6.67}$ was also performed on $YBa_2Cu_3O_{6.75}$ (during a different experiment run and in a different magnet, hence the different temperatures and maximum field).

Figure S3 shows the raw frequency-shift data for $YBa_2Cu_3O_{6.75}$ at each temperature, along with the polynomial background in black and the full fit to Equation S5 in red. The fits yield $F = 569 \pm 4$ T, $\Delta F = 19 \pm 7$ T, $\tau = 0.06 \pm 0.02$ ps, and $m^\star = 2.1 \pm 0.1$ m_e. At 70 T these parameters yield $\omega_c\tau \approx 0.5$, consistent with oscillations becoming visible near this field. While the shape of the background evolves with increasing temperature (due to the temperature dependence of the non-oscillatory magnetoresistance), it remains smooth and non-oscillatory at all temperatures. The background-free data from these fits, along with the mass fit from the oscillation amplitude, is shown in Figure S4.

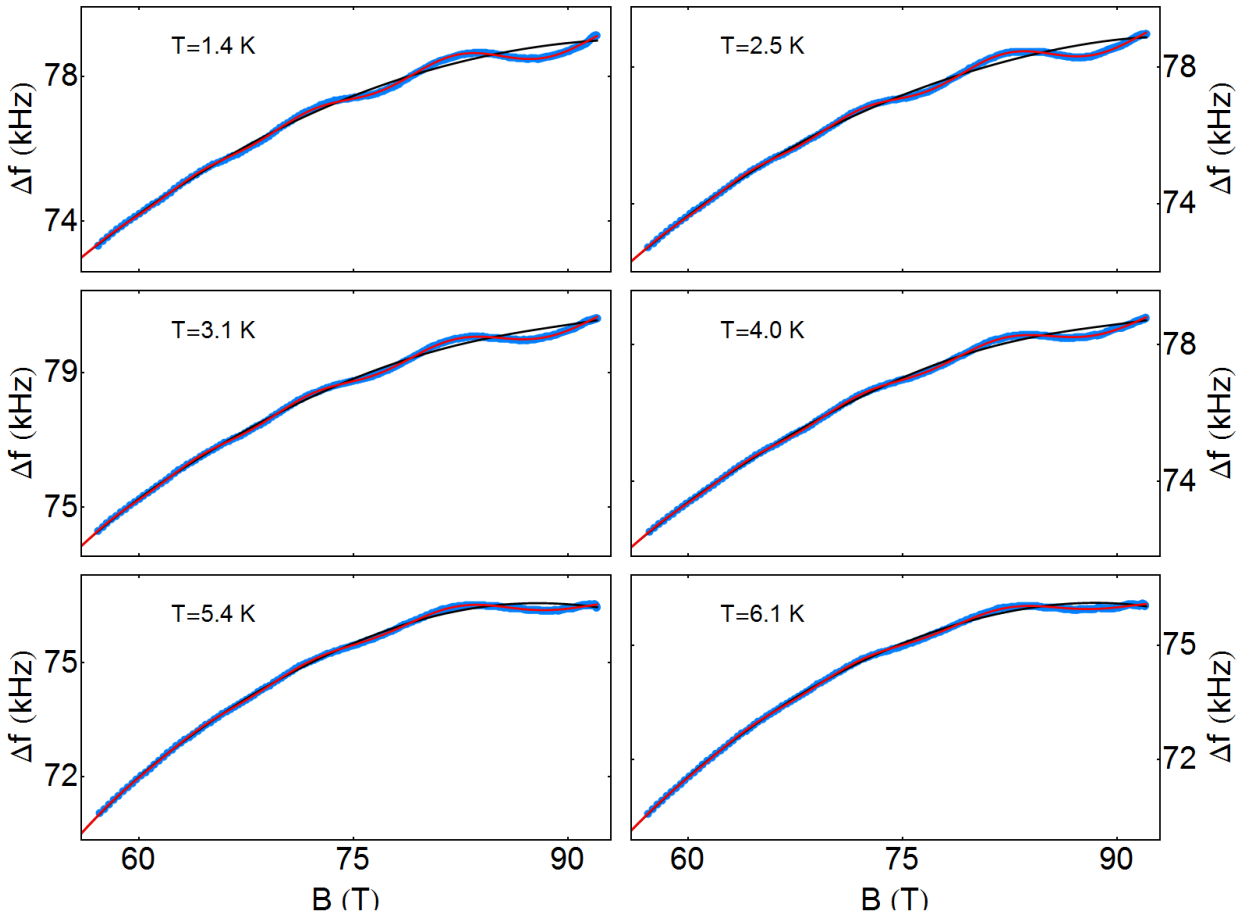


Fig. S3: Shift in the proximity-diode oscillator frequency for $YBa_2Cu_3O_{6.75}$, proportional to the skin depth (and therefore resistivity) at ~ 30 MHz: the raw data is in blue; the fit to Equation S2 plus a background is in red; the background alone is in black. All panels have the same vertical span.

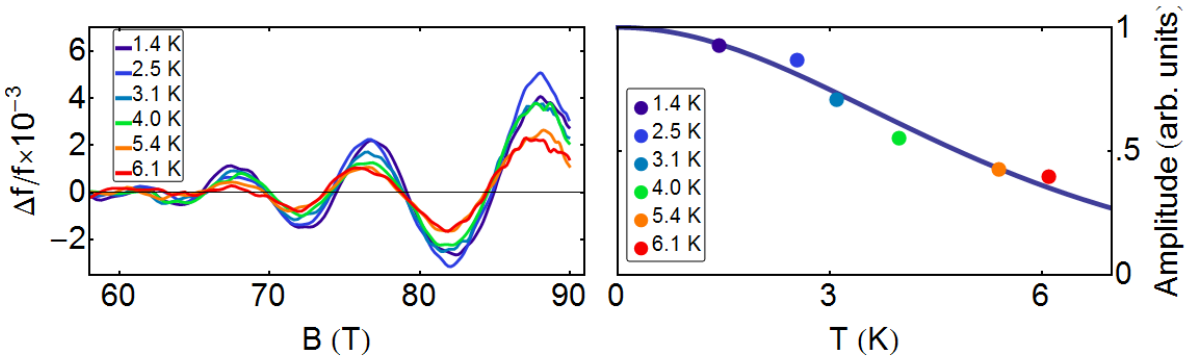


Fig. S4: *Left panel:* Relative frequency shift with respect to the background, proportional to $\Delta\rho/\rho$, $YBa_2Cu_3O_{6.75}$ at each temperature with a background subtracted. *Right panel:* Fit to the oscillation amplitude, yielding $m^\star = 2.1 \pm 0.1$.

$YBa_2Cu_3O_{6.80}$

Shubnikov-de Haas oscillations were measured in the $\hat{c}$-axis resistivity of $YBa_2Cu_3O_{6.80}$. Sample contacts were prepared in a Corbino-like geometry, with large current contacts on both faces and small voltage contacts in the centre (see **(author?)** [62] for sample preparation details). Approximately 3 mA of current was driven through the sample at 500 kHz, and the voltage signal across the sample was recorded at 20 MHz using a digitizer. The data was then processed with a digital lock-in amplifier. Figure S5 shows the raw magnetoresistance data for $YBa_2Cu_3O_{6.80}$ at each temperature, plus the polynomial background in black and the full fit to Equation S5 in red. The fits yield $F = 565 \pm 8$ T, $\Delta F = 21 \pm 8$ T, $\tau = 0.09 \pm 0.02$ ps, and $m^\star = 2.4 \pm 0.2$ m_e. The data with the background removed, along with the mass fit, is shown in Figure S6.

The derivative of the magnetoresistance for $YBa_2Cu_3O_{6.80}$ is shown in Figure S7, along with the background in black, plus the full fit in red. The background-free data is shown in Figure S8, along with the mass fit which gives $m^\star = 2.5 \pm 0.2$: consistent with $m^\star = 2.4 \pm 0.2$ obtained using the un-differentiated data.

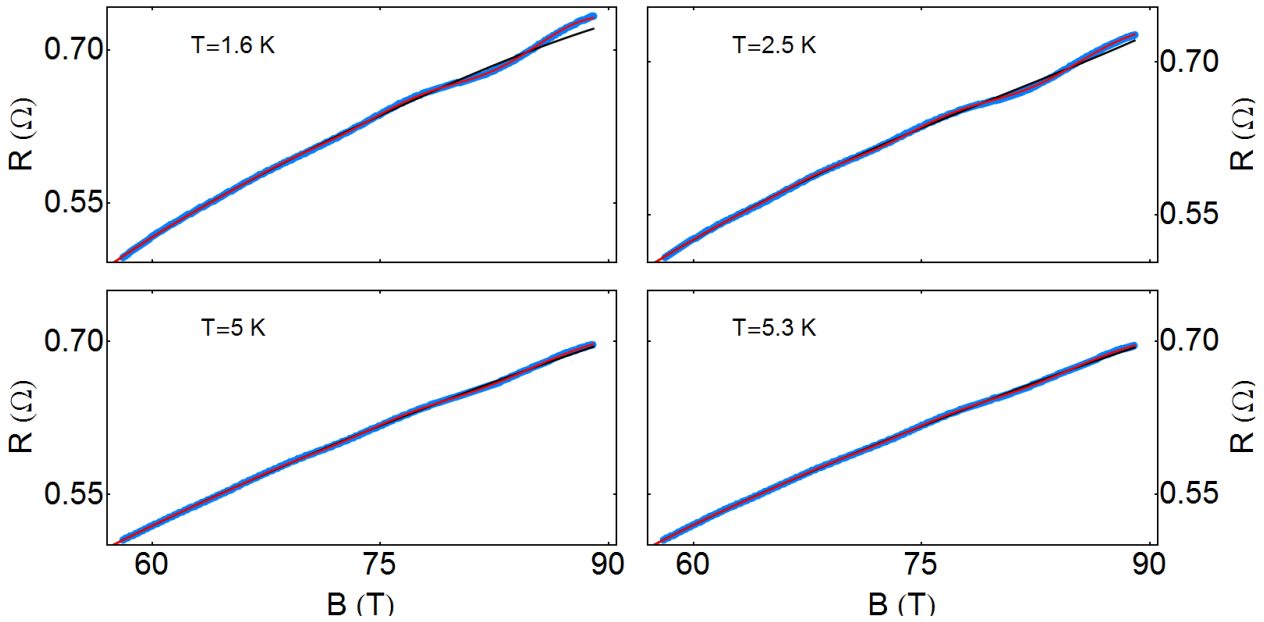


Fig. S5: $\hat{c}$-axis magnetotransport for $YBa_2Cu_3O_{6.80}$: the raw data is in blue; the fit to Equation S2 plus a background is in red; the background alone is in black. All panels have the same vertical span.

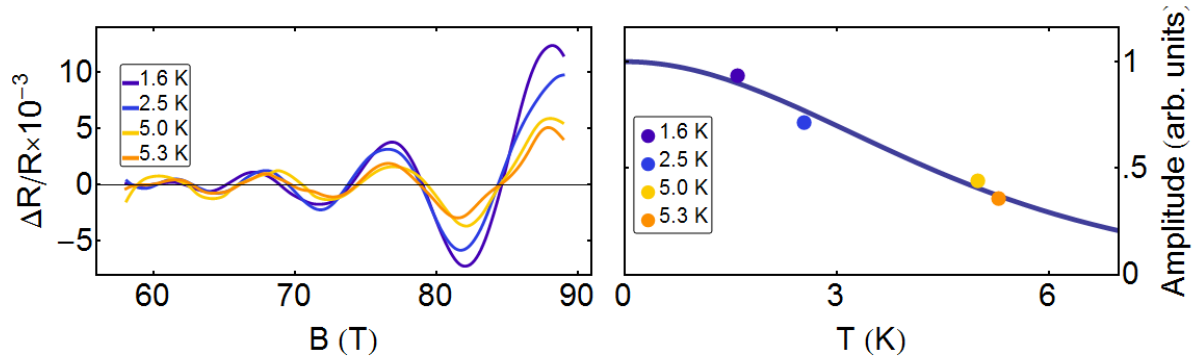


Fig. S6: *Left panel:* Magnetoresistance for $YBa_2Cu_3O_{6.80}$ at each temperature with a background subtracted. *Right panel:* Fit to the oscillation amplitude, yielding $m^\star = 2.4 \pm 0.2$.

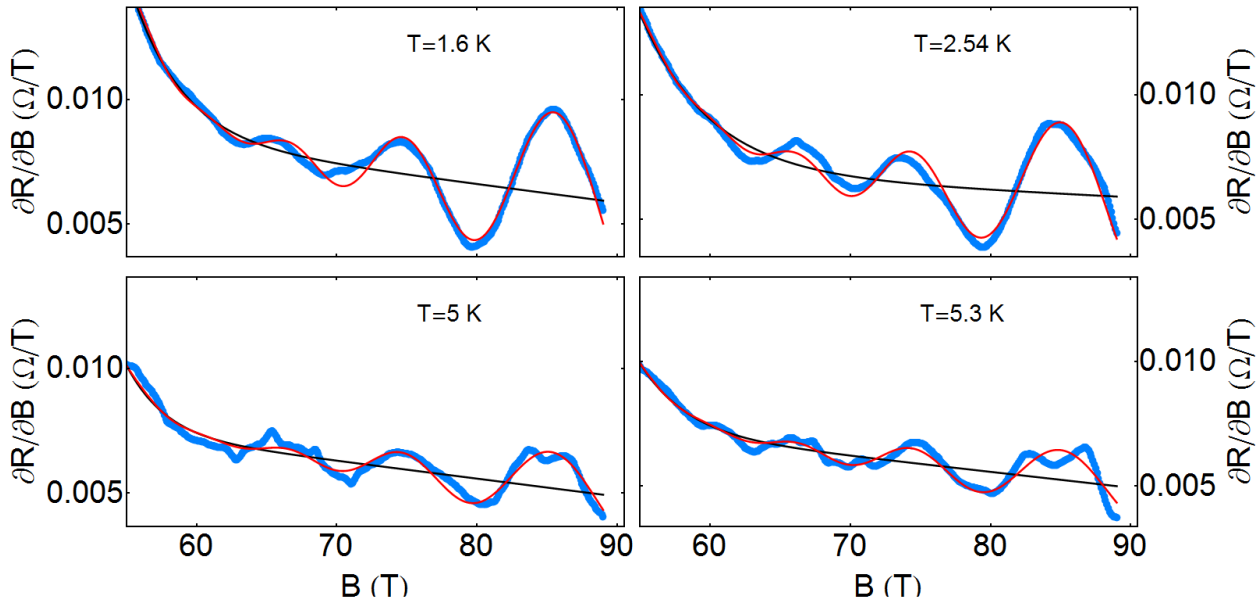


Fig. S7: Derivative of the magnetoresistance for $YBa_2Cu_3O_{6.80}$: the raw data is in blue; the fit to Equation S2 plus a background is in red; the background alone is in black. All panels have the same vertical span.

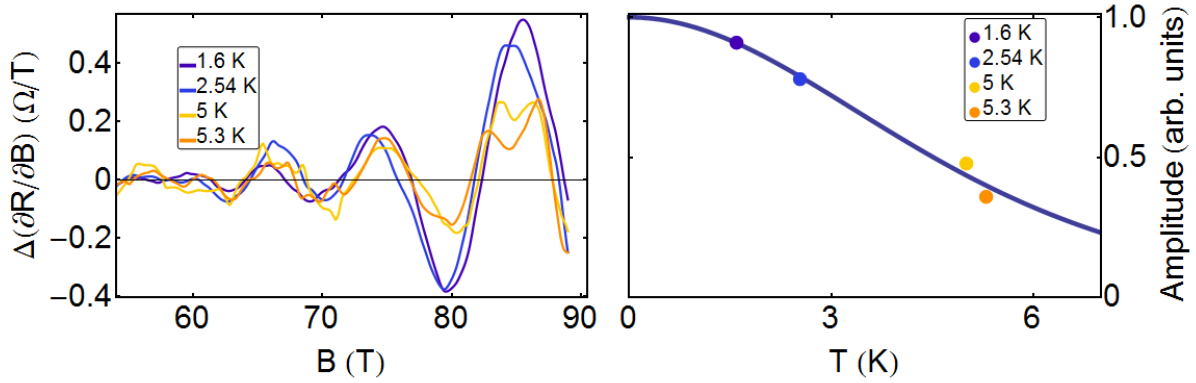


Fig. S8: *Left panel:* Derivative of the magnetoresistance for $YBa_2Cu_3O_{6.80}$ at each temperature with a background subtracted. *Right panel:* Fit to the oscillation amplitude, yielding $m^\star = 2.5 \pm 0.2$.

$YBa_2Cu_3O_{6.86}$

The same magnetotransport technique that was performed on $YBa_2Cu_3O_{6.80}$ was also performed on $YBa_2Cu_3O_{6.86}$ (during a different experiment run, hence the different temperatures).

Figure S11 shows the raw magnetoresistance data for $YBa_2Cu_3O_{6.86}$, along with a fit in red and the background in black. The fits yield $F = 599\pm12$ T, $\Delta F = 21\pm10$ T, $\tau = 0.07\pm0.03$ ps, and $m^\star = 3.6\pm0.2$ m_e. To emphasise that the background at each temperature is non-oscillatory, the derivative of the background is plotted in the right panel of Figure S10.

The derivative of the magnetoresistance for $YBa_2Cu_3O_{6.86}$ is shown in Figure S12, along with the background in black, plus the full fit in red. Here, the oscillations can clearly be seen in the derivative at all temperatures. The background-free data is shown in Figure S13, along with the mass fit which gives $m^\star = 3.4 \pm 0.2$: consistent with the mass of $m^\star = 3.6 \pm 0.2$ obtained using the un-differentiated data.

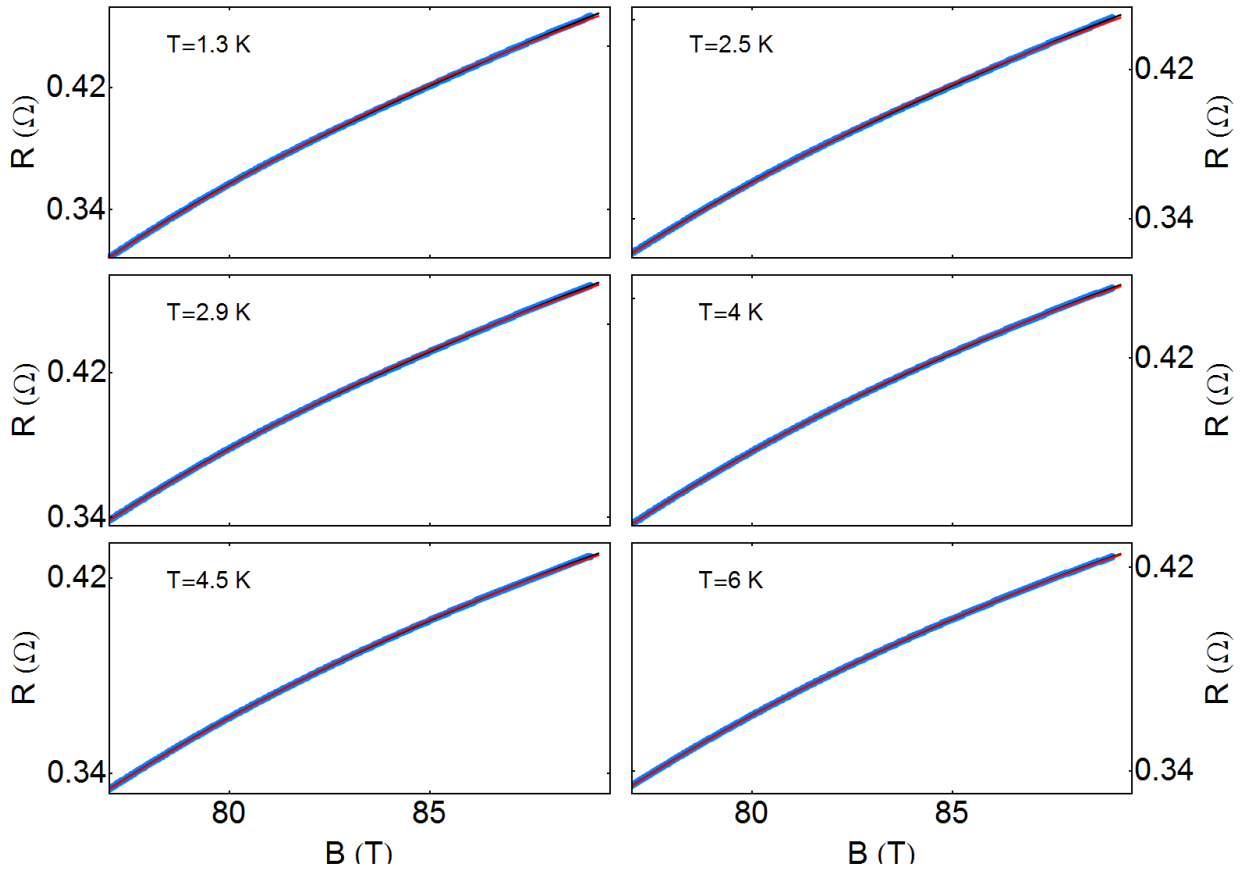


Fig. S9: Magnetoresistance for $YBa_2Cu_3O_{6.86}$: the raw data is in blue; the fit to Equation S1 plus a background is in red; the background alone is in black. All panels have the same vertical span.

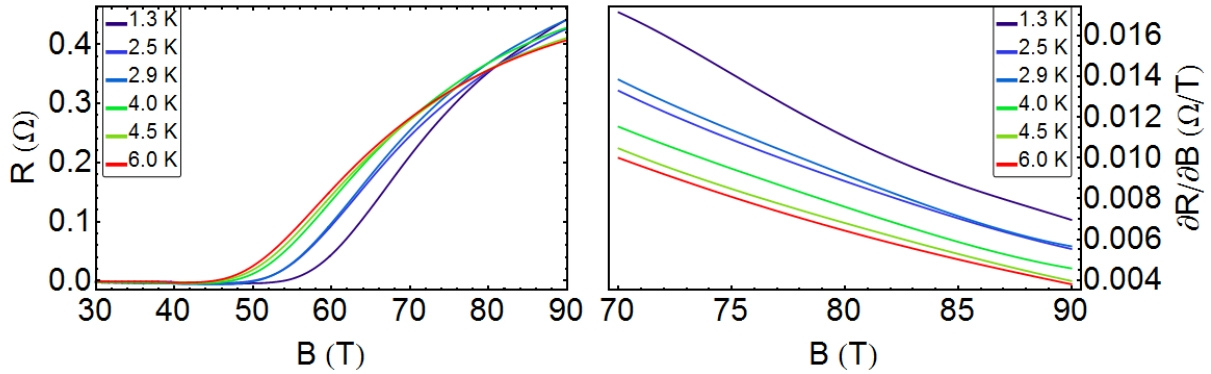


Fig. S10: *Left panel:* raw magnetoresistance for $YBa_2Cu_3O_{6.86}$ across the entire field and temperature range. *Right panel:* derivative of the background, shown in black in Figure S9, used to extract the oscillatory component of the magnetoresistance, show in the left panel of Figure S11.

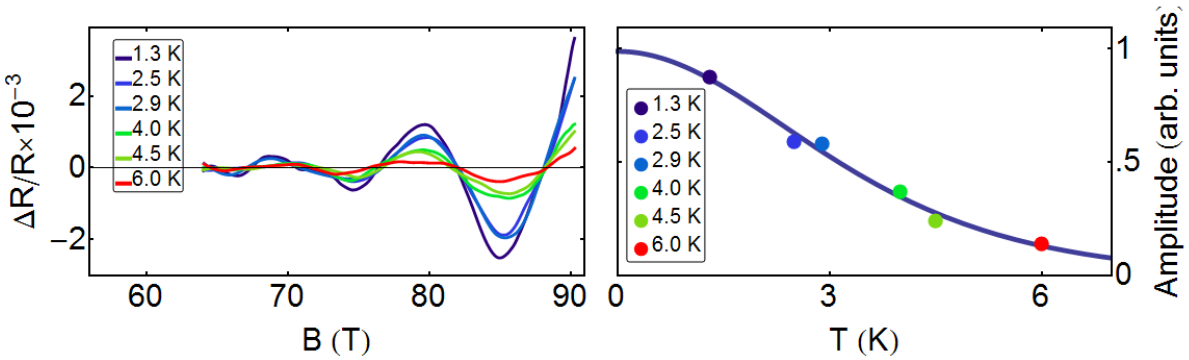


Fig. S11: *Left panel:* the magnetoresistance for $YBa_2Cu_3O_{6.86}$ at each temperature with a background subtracted (see Figure S11). *Right panel:* Fit to the oscillation amplitude, yielding $m^\star = 3.6 \pm 0.2$.

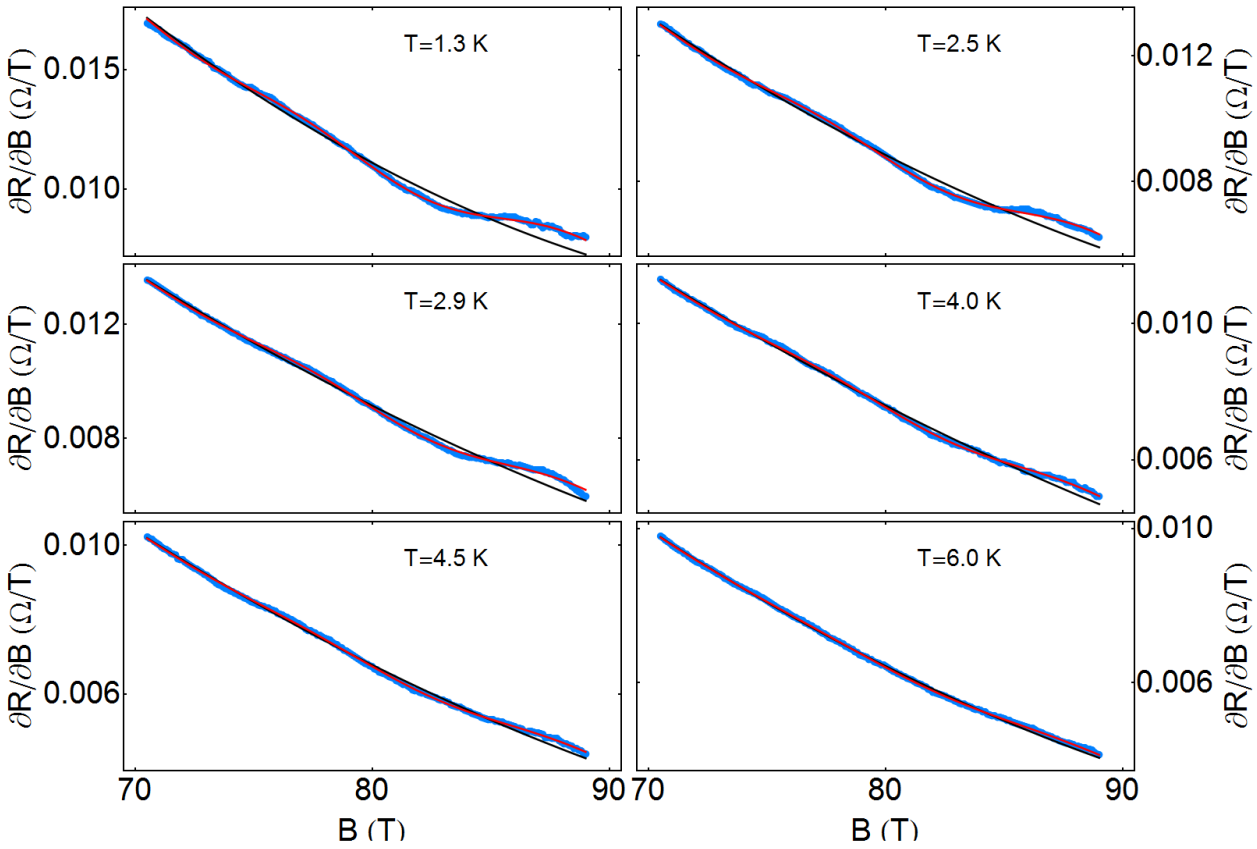


Fig. S12: Derivative of the magnetoresistance for $YBa_2Cu_3O_{6.86}$: the raw data is in blue; the fit to Equation S1 plus a background is in red; the background alone is in black. All panels have the same vertical span.

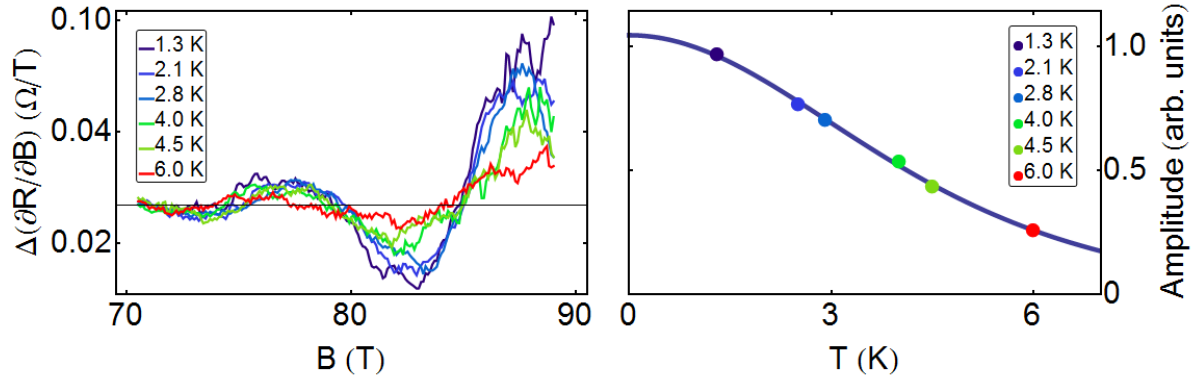


Fig. S13: *Left panel:* derivative of the magnetoresistance for $YBa_2Cu_3O_{6.86}$ at each temperature with a background subtracted (see Figure S5). *Right panel:* Fit to the oscillation amplitude, yielding $m^\star = 3.4 \pm 0.2$, in agreement with the mass reported in the main text.

Rising and falling field

In a pulsed field environment where $\partial B/\partial t$ exceeds 10^4 T/s (see Figure S14), sample self-heating can become an issue. For high-T_c superconductors, the melting of the vortex lattice as the sample enters the resistive state dissipates heat in the sample. While this heating is unavoidable, the sample can usually equilibrate with the high-thermal-conductivity sapphire sample platform by peak field, and the data on falling field is then taken at a constant and known temperature. This condition is checked by looking for

hysteresis at high field: if the sample has come to equilibrium by peak field, it will show no hysteresis here. This is particularly important above 4 K when the sample is in gas, rather than liquid. This procedure has been validated by obtaining the same mass at the same doping ($YBa_2Cu_3O_{6.58}$) in magnets of different pulse length (including the DC hybrid in Tallahassee).

Figure S15 shows the two extremes of temperatures for $YBa_2Cu_3O_{6.86}$: the doping where the resistive transition occurs at the highest field and equilibration time is therefore shortest. There is some heating when the resistive state is entered at both temperatures (rising data is in lighter shades), but by ∼75 T the hysteresis is gone, indicating thermal equilibrium. Also note that the heating is the same in the liquid (1.3 K) as it is in the gas (6 K). The size of the hysteresis at the melting transition in Figure S15, before the sample reaches thermal equilibrium, corresponds to heating of about 1 K (see [57]). We are therefore in the regime where the sample comes to equilibrium before peak field, and thus sample self-heating during the pulse is not a significant source of error in this experiment.

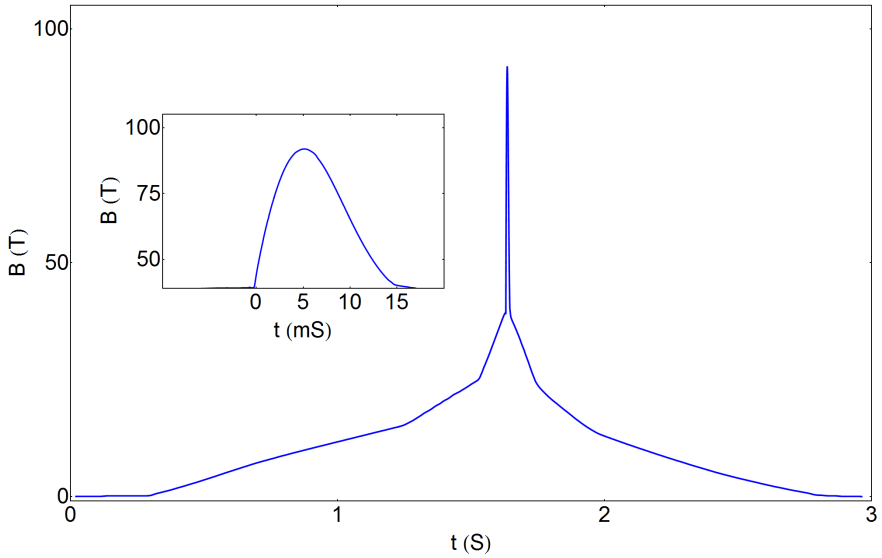


Fig. S14: Field profile of the pulsed magnet used in this experiment. The "outsert" generator-driven magnet is ramped with a shaped waveform over 1.5 seconds to 40 T, at which point the "insert" capacitor-bank driven magnet is fired to 52 T, combining for 92 T at the center of the bore of the magnet.

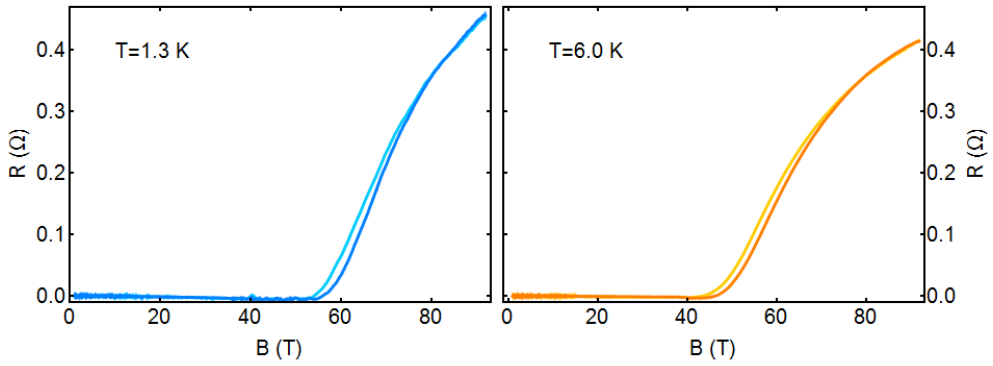


Fig. S15: Rising (light shades) and falling (dark shades) field resistance for $YBa_2Cu_3O_{6.86}$ at the highest (6 K) and lowest (1.3 K) temperatures. The data here was analysed with time constant of $2\mu s$ to avoid broadening the resistive transition on rising field. This is shorter than the $300\mu s$ used for Figure S9 and Figure S12, where only falling field data is shown.

Physical properties at a quantum critical point

An enhancement of the thermodynamic effective mass $m^\star$ at a quantum critical point is often accompanied by an enhancement of other physical properties that depend on the mass (density of states), including, but not limited to, the upper critical field, the superconducting condensation energy, the London penetration depth, the residual specific heat "γ", the "A" coefficient of the T^2 term in the resistivity, and the residual resistivity "ρ_0" at $T = 0$ [63, 64, 65, 42, 66, 5]. Not all techniques show the same mass enhancement within a given material: the thermodynamic mass as measured by quantum oscillations in $CeRh_2Si_2$, and the specific heat γ, are enhanced by a factor of four approaching the critical pressure [63, 42], while the square root of the A coefficient ($A \propto (m^\star)^2$) is enhanced by a factor of 3 over the same pressure range [42]; the thermodynamic mass in $CeRhIn_5$ is enhanced by a factor of 10 [3], the specific heat γ by a factor of ~ 6 [64], the square root of H_{c2} ($H_{c2} \propto (m^\star)^2$) by a factor of ≈ 2 [66], and the mass estimated from the slope of H_{c2} as a function of T_c (as tuned with pressure) by less than a factor of two [66]; the specific heat and penetration depth in $BaFe_2(As_{1-x}P_x)_2$ show the same mass enhancement at the quantum critical point, but differ by a factor of two at $x \approx 0.4$ [5]. These differences in the apparent mass enhancement are not unexpected: each physical property is sensitive to different renormalizations. For example, the the mass measured in cyclotron resonance experiments is not enhanced by electron-electron interactions [67], the spin susceptibility is not enhanced by electron-phonon interactions [68], and penetration depth probes the "dynamic effective mass", $\frac{m^\star}{1+\frac{1}{3}F_1}$ [44]. For a review of the many different "masses" in metals see [44], section IV. Additionally the theories used to extract mass may not valid near a quantum critical point (or at any pressure/doping in an unconventional metal), for example, the BCS expression relating H_{c2} and $m^\star$, $H_{c2} = \frac{\Phi_0}{2\pi}\left(\frac{\pi\Delta(0)m^\star}{\hbar^2 k_F}\right)^2$, will undoubtedly fail near a QCP in a non-BCS superconductor (and may only be qualitatively correct even away from the QCP).

It must be emphasized that none of these properties truly "diverges" at the QCP, but instead reaches a maximum there. There are several possible explanations for this: suppression and broadening of the enhancement at the QCP due to sample inhomogeneity; the breakdown of the theories used to extract mass near the QCP, as mentioned above; the introduction of an energy scale into the system, such as a superconducting gap, that serves to cut off the fluctuating mode that is renormalizing the mass.

In the case of $YBa_2Cu_3O_{6+\delta}$, both H_{c2} [39] and the heat capacity jump at T_c ($\Delta\gamma$) [40, 41] show maxima near $p_{crit} \approx 0.18$ and $p_{crit} \approx 0.08$, as shown in Figure 1 of the main text. Both of these observations are consistent with the mass being enhanced at the quantum critical point at $p_{crit} \approx 0.18$. Superfluid density, as measured by μSR, on the other hand, does not show any maxima [43] (previous measurements that do show a peak in superfluid density near $p_{crit} \approx 0.18$ have been disputed due to the introduction of zinc into these samples, which is known to be a strong breaker of Cooper pairs [69]). A systematic doping dependence of the normal-state γ in $YBa_2Cu_3O_{6+\delta}$ has not been performed, due to the extreme magnetic fields needed to access the normal state. The differences in mass enhancement seen by different probes in the cuprates may contain valuable information regarding how interactions dress the quasiparticles, and warrants further investigation.

References

[1] P Coleman, C Pepin, QM Si, and R Ramazashvili. How do fermi liquids get heavy and die? *Journal of Physics-Condensed Matter*, 13(35):R723–R738, Sep 3 2001.

[2] Louis Taillefer. Scattering and pairing in cuprate superconductors. In *Annual Review of Condensed Matter Physics, Vol 1*, volume 1 of *Annual Review of Condensed Matter Physics*, pages 51–70. 2010.

[3] H Shishido, R Settai, H Harima, and Y Onuki. A drastic change of the fermi surface at a critical pressure in CeRhIn5: dHvA study under pressure. *Journal of the Physical Society of Japan*, 74(4):1103–1106, Apr 2005.

[4] Philipp Gegenwart, Qimiao Si, and Frank Steglich. Quantum criticality in heavy-fermion metals. *Nature Physics*, 4(3):186–197, Mar 2008.

[5] P. Walmsley, C. Putzke, L. Malone, I. Guillamon, D. Vignolles, C. Proust, S. Badoux, A. I. Coldea, M. D. Watson, S. Kasahara, Y. Mizukami, T. Shibauchi, Y. Matsuda, and A. Carrington. Quasiparticle mass enhancement close to the quantum critical point in $BaFe_2(As_{1-x}P_x)_2$. *Physical Review Letters*, 110(25), Jun 21 2013.

[6] P. Monthoux, D. Pines, and G. G. Lonzarich. Superconductivity without phonons. *Nature*, 450(7173):1177–1183, Dec 20 2007.

[7] PW Anderson, PA Lee, M Randeria, TM Rice, N Trivedi, and FC Zhang. The physics behind high-temperature superconducting cuprates: the 'plain vanilla' version of RVB. *Journal of Physics-Condensed Matter*, 16(24):R755–R769, Jun 23 2004.

[8] JL Tallon and JW Loram. The doping dependence of T* - what is the real high-T-c phase diagram? *Physica C*, 349(1-2):53–68, Jan 1 2001.

[9] G. S. Boebinger, Yoichi Ando, A. Passner, T. Kimura, M. Okuya, J. Shimoyama, K. Kishio, K. Tamasaku, N. Ichikawa, and S. Uchida. Insulator-to-metal crossover in the normal state of $La_{2-x}Sr_xCuO_4$ near optimum doping. *Phys. Rev. Lett.*, 77:5417–5420, Dec 1996.

[10] Yoichi Ando, Kouji Segawa, Seiki Komiya, and A. N. Lavrov. Electrical resistivity anisotropy from self-organized one dimensionality in high-temperature superconductors. *Phys. Rev. Lett.*, 88:137005, Mar 2002.

[11] Fedor F Balakirev, Jonathan B Betts, Albert Migliori, S Ono, Yoichi Ando, and Gregory S Boebinger. Signature of optimal doping in Hall-effect measurements on a high-temperature superconductor. *Nature*, 424(6951):912–915, 2003.

[12] B. Fauqué, Y. Sidis, V. Hinkov, S. Pailhès, C. T. Lin, X. Chaud, and P. Bourges. Magnetic order in the pseudogap phase of High-T_C superconductors. *Phys. Rev. Lett.*, 96:197001, May 2006.

[13] Jing Xia, Elizabeth Schemm, G. Deutscher, S. A. Kivelson, D. A. Bonn, W. N. Hardy, R. Liang, W. Siemons, G. Koster, M. M. Fejer, and A. Kapitulnik. Polar kerr-effect measurements of the high-temperature YBa(2)Cu(3)O(6+x) superconductor: Evidence for broken symmetry near the pseudogap temperature. *Physical Review Letters*, 100(12), Mar 28 2008.

[14] A. Shekhter, B. J. Ramshaw, R. D. McDonald, J. B. Betts, F. Balakirev, Ruixing Liang, W. N. Hardy, D. A. Bonn, Scott C. Riggs, and Albert Migliori. Bounding the pseudogap with a line of phase transitions in $YBa_2Cu_3O_{6+\delta}$. *Nature*, 498(7452):75–77, 2013.

[15] S. Blanco-Canosa, A. Frano, T. Loew, Y. Lu, J. Porras, G. Ghiringhelli, M. Minola, C. Mazzoli, L. Braicovich, E. Schierle, E. Weschke, M. Le Tacon, and B. Keimer. Momentum-dependent charge correlations in YBa2Cu3O6+δ superconductors probed by resonant x-ray scattering: Evidence for three competing phases. *Physical Review Letters*, 110(18), May 1 2013.

[16] K Fujita, Chung Koo Kim, Inhee Lee, Jinho Lee, MH Hamidian, IA Firmo, S Mukhopadhyay, H Eisaki, S Uchida, MJ Lawler, et al. Simultaneous transitions in cuprate momentum-space topology and electronic symmetry breaking. *Science*, 344(6184):612–616, 2014.

[17] CM Varma. Pseudogap phase and the quantum-critical point in copper-oxide metals. *Physical Review Letters*, 83(17):3538–3541, OCT 25 1999.

[18] S Chakravarty, RB Laughlin, DK Morr, and C Nayak. Hidden order in the cuprates. *Physical Review B*, 63(9), MAR 1 2001.

[19] Subir Sachdev. *Quantum phase transitions*. Wiley Online Library, 2007.

[20] Patrick A. Lee. From high temperature superconductivity to quantum spin liquid: progress in strong correlation physics. *Reports on Progress in Physics*, 71(1), Jan 2008.

[21] SA Kivelson, E Fradkin, and VJ Emery. Electronic liquid-crystal phases of a doped Mott insulator. *Nature*, 393(6685):550–553, Jun 11 1998.

[22] R. Daou, J. Chang, David LeBoeuf, Olivier Cyr-Choinière, Francis Laliberte, Nicolas Doiron-Leyraud, B. J. Ramshaw, Ruixing Liang, D. A. Bonn, W. N. Hardy, and Louis Taillefer. Broken rotational symmetry in the pseudogap phase of a high-T_c superconductor. *Nature*, 463(7280):519–522, Jan 28 2010.

[23] B. J. Ramshaw, Baptiste Vignolle, James Day, Ruixing Liang, W. N. Hardy, Cyril Proust, and D. A. Bonn. Angle dependence of quantum oscillations in $YBa_2Cu_3O_{6.59}$ shows free-spin behaviour of quasiparticles. *Nature Physics*, 7(3):234–238, Mar 2011.

[24] G. Ghiringhelli, M. Le Tacon, M. Minola, S. Blanco-Canosa, C. Mazzoli, N. B. Brookes, G. M. De Luca, A. Frano, D. G. Hawthorn, F. He, T. Loew, M. Moretti Sala, D. C. Peets, M. Salluzzo, E. Schierle, R. Sutarto, G. A. Sawatzky, E. Weschke, B. Keimer, and L. Braicovich. Long-range incommensurate charge fluctuations in (Y,Nd)Ba2Cu3O6+x. *Science*, 337(6096):821–825, 2012.

[25] J. Chang, A. T. Blackburn, N. B. Holmes, J. Christensen, J. Larsen, J. Mesot, Ruixing Liang, D. A. Bonn, W. N. Hardy, A. Watenphul, M. v. Zimmerman, E. M. Forgan, and S. M. Hayden. Direct observation of competition between superconductivity and charge density wave order in $YBa_2Cu_3O_y$. *Nature Physics*, Oct 2012.

[26] Tao Wu, Hadrien Mayaffre, Steffen Krämer, Mladen Horvatić, Claude Berthier, Philip L Kuhns, Arneil P Reyes, Ruixing Liang, WN Hardy, DA Bonn, et al. Emergence of charge order from the vortex state of a high-temperature superconductor. *Nature communications*, 4, 2013.

[27] Markus Huecker, Niels Bech Christensen, AT Holmes, Elizabeth Blackburn, EM Forgan, Ruixing Liang, DA Bonn, WN Hardy, Olof Gutowski, M v Zimmermann, et al. Competing charge, spin, and superconducting orders in underdoped YBa2Cu3Oy. *Physical Review B*, 90(5):054514, 2014.

[28] R. Comin, A. Frano, M. M. Yee, Y. Yoshida, H. Eisaki, E. Schierle, E. Weschke, R. Sutarto, F. He, A. Soumyanarayanan, Yang He, M. Le Tacon, I. S. Elfimov, Jennifer E. Hoffman, G. A. Sawatzky, B. Keimer, and A. Damascelli. Charge order driven by fermi-arc instability in Bi2Sr2-xLaxCuO6+δ. *Science*, 343(6169):390–392, Jan 24 2014.

[29] D. Shoenberg. *Magnetic oscillations in metals*. Cambridge monographs on physics. Cambridge University Press, 1984.

[30] Nicolas Doiron-Leyraud, Cyril Proust, David LeBoeuf, Julien Levallois, Jean-Baptiste Bonnemaison, Ruixing Liang, D. A. Bonn, W. N. Hardy, and Louis Taillefer. Quantum oscillations and the fermi surface in an underdoped high-Tc superconductor. *Nature*, 447(7144):565–568, May 31 2007.

[31] David LeBoeuf, Nicolas Doiron-Leyraud, Julien Levallois, R. Daou, J.-B. Bonnemaison, N. E. Hussey, L. Balicas, B. J. Ramshaw, Ruixing Liang, D. A. Bonn, W. N. Hardy, S. Adachi, Cyril Proust, and Louis Taillefer. Electron pockets in the fermi surface of hole-doped high-T-c superconductors. *Nature*, 450(7169):533–536, Nov 22 2007.

[32] E. A. Yelland, J. Singleton, C. H. Mielke, N. Harrison, F. F. Balakirev, B. Dabrowski, and J. R. Cooper. Quantum oscillations in the underdoped cuprate $YBa_2Cu_4O_8$. *Phys. Rev. Lett.*, 100:047003, Feb 2008.

[33] A. F. Bangura, J. D. Fletcher, A. Carrington, J. Levallois, M. Nardone, B. Vignolle, P. J. Heard, N. Doiron-Leyraud, D. LeBoeuf, L. Taillefer, S. Adachi, C. Proust, and N. E. Hussey. Small fermi surface pockets in underdoped high temperature superconductors: Observation of shubnikov-de haas oscillations in YBa(2)Cu(4)O(8). *Physical Review Letters*, 100(4), FEB 1 2008.

[34] Neven Barišić, Sven Badoux, Mun K Chan, Chelsey Dorow, Wojciech Tabis, Baptiste Vignolle, Guichuan Yu, Jérôme Béard, Xudong Zhao, Cyril Proust, and Martin Greven. Universal quantum oscillations in the underdoped cuprate superconductors. *Nature Physics*, 9(12):761–764, 2013.

[35] B. Vignolle, A. Carrington, R. A. Cooper, M. M. J. French, A. P. Mackenzie, C. Jaudet, D. Vignolles, Cyril Proust, and N. E. Hussey. Quantum oscillations in an overdoped high-T_c superconductor. *Nature*, 455(7215):952–955, Oct 16 2008.

[36] Materials and Methods, Supplementary Text, and Supplementary Figures are available as supporting material on Science Online.

[37] Suchitra E. Sebastian, N. Harrison, M. M. Altarawneh, Ruixing Liang, D. A. Bonn, W. N. Hardy, and G. G. Lonzarich. Fermi-liquid behavior in an underdoped high-T_c superconductor. *Phys. Rev. B*, 81:140505, Apr 2010.

[38] Z-X Shen, A Lanzara, S Ishihara, and N Nagaosa. Role of the electron-phonon interaction in the strongly correlated cuprate superconductors. *Philosophical Magazine B*, 82(13):1349–1368, 2002.

[39] G Grissonnanche, O Cyr-Choiniere, F Laliberte, S Rene de Cotret, A Juneau-Fecteau, S Dufour-Beausejour, M-E Delage, D LeBoeuf, J Chang, B.J. Ramshaw, D. A. Bonn, W. N. Hardy, Ruixing Liang, S. Adachi, N. E. Hussey, B. Vignolle, C. Proust, M. Sutherland, S. Kramer, J.-H. Park, D. Graf, N. Doiron-Leyraud, and Louis. Taillefer. Direct measurement of the upper critical field in a cuprate superconductor. *Nature Communications*, 5, Feb 2014.

[40] J. W. Loram, K. A. Mirza, J. R. Cooper, and W. Y. Liang. Electronic specific heat of $YBa_2Cu_3O_{6+x}$ from 1.8 to 300 k. *Phys. Rev. Lett.*, 71:1740–1743, Sep 1993.

[41] JW Loram, KA Mirza, JR Cooper, and JL Talloon. Specific heat evidence on the normal state pseudogap. *Journal of Physics and Chemistry of Solids*, 59(10-12):2091–2094, Oct-Dec 1998. International Conference on Spectroscopies in Novel Superconductors (SNS'97), Cape Cod, MA, Sep 14-18, 1997.

[42] Rikio Settai, Tetsuya Takeuchi, and Yoshichika Ōnuki. Recent advances in Ce-based heavy-fermion superconductivity and fermi surface properties. *Journal of the Physical Society of Japan*, 76(5), 2007.

[43] J. E. Sonier, S. A. Sabok-Sayr, F. D. Callaghan, C. V. Kaiser, V. Pacradouni, J. H. Brewer, S. L. Stubbs, W. N. Hardy, D. A. Bonn, R. Liang, and W. A. Atkinson. Hole-doping dependence of the magnetic penetration depth and vortex core size in $YBa_2Cu_3O_y$: Evidence for stripe correlations near $\frac{1}{8}$ hole doping. *Phys. Rev. B*, 76:134518, Oct 2007.

[44] AJ Leggett. Inequalities instabilites and renormalization in metals and other fermi liquids. *Annals of Physics*, 46(1):76–&, 1968.

[45] M. Huecker, M. v. Zimmermann, G. D. Gu, Z. J. Xu, J. S. Wen, Guangyong Xu, H. J. Kang, A. Zheludev, and J. M. Tranquada. Stripe order in superconducting La2-xBaxCuO4 (0.095 <= x <= 0.155). *Physical Review B*, 83(10), Mar 17 2011.

[46] Suchitra E. Sebastian, N. Harrison, M. M. Altarawneh, C. H. Mielke, Ruixing Liang, D. A. Bonn, W. N. Hardy, and G. G. Lonzarich. Metal-insulator quantum critical point beneath the high T_c superconducting dome. *Proceedings of the National Academy of Sciences of the United States of America*, 107(14):6175–6179, APR 6 2010.

[47] HQ Yuan, FM Grosche, M Deppe, C Geibel, G Sparn, and F Steglich. Observation of two distinct superconducting phases in CeCu2Si2. *Science*, 302(5653):2104–2107, Dec 19 2003.

[48] M. Le Tacon, G. Ghiringhelli, J. Chaloupka, M. Moretti Sala, V. Hinkov, M. W. Haverkort, M. Minola, M. Bakr, K. J. Zhou, S. Blanco-Canosa, C. Monney, Y. T. Song, G. L. Sun, C. T. Lin, G. M. De Luca, M. Salluzzo, G. Khaliullin, T. Schmitt, L. Braicovich, and B. Keimer. Intense paramagnon excitations in a large family of high-temperature superconductors. *Nature Physics*, 7(9):725–730, Sep 2011.

[49] David LeBoeuf, Nicolas Doiron-Leyraud, B. Vignolle, Mike Sutherland, B. J. Ramshaw, J. Levallois, R. Daou, Francis Laliberté, Olivier Cyr-Choinière, Johan Chang, Y. J. Jo, L. Balicas, Ruixing Liang, D. A. Bonn, W. N. Hardy, Cyril Proust, and Louis Taillefer. Lifshitz critical point in the cuprate superconductor $YBa_2Cu_3O_y$ from high-field hall effect measurements. *Phys. Rev. B*, 83:054506, Feb 2011.

[50] Laimei Nie, Gilles Tarjus, and Steven Allan Kivelson. Quenched disorder and vestigial nematicity in the pseudogap regime of the cuprates. *Proceedings of the National Academy of Sciences of the United States of America*, 111(22):7980–7985, JUN 3 2014.

[51] David LeBoeuf, S. Kraemer, W. N. Hardy, Ruixing Liang, D. A. Bonn, and Cyril Proust. Thermodynamic phase diagram of static charge order in underdoped YBa2Cu3Oy. *Nature Physics*, 9(2):79–83, Feb 2013.

[52] Baptiste Vignolle, David Vignolles, David LeBoeuf, Stephane Lepault, Brad Ramshaw, Ruixing Liang, D. A. Bonn, W. N. Hardy, Nicolas Doiron-Leyraud, A. Carrington, N. E. Hussey, Louis Taillefer, and Cyril Proust. Quantum oscillations and the fermi surface of high-temperature cuprate superconductors. *Comptes Rendus Physique*, 12(5-6):446–460, Jun-Aug 2011.

[53] John Singleton, Clarina de la Cruz, R. D. McDonald, Shiliang Li, Moaz Altarawneh, Paul Goddard, Isabel Franke, Dwight Rickel, C. H. Mielke, Xin Yao, and Pengcheng Dai. Magnetic quantum oscillations in $YBa_2Cu_3O_{6.61}$ and $YBa_2Cu_3O_{6.69}$ in fields of up to 85 T: Patching the hole in the roof of the superconducting dome. *Phys. Rev. Lett.*, 104:086403, Feb 2010.

[54] F. Coneri, S. Sanna, K. Zheng, J. Lord, and R. De Renzi. Magnetic states of lightly hole-doped cuprates in the clean limit as seen via zero-field muon spin spectroscopy. *Phys. Rev. B*, 81:104507, Mar 2010.

[55] Y Ando, S Komiya, K Segawa, S Ono, and Y Kurita. Electronic phase diagram of high-T-c cuprate superconductors from a mapping of the in-plane resistivity curvature. *Physical Review Letters*, 93(26), Dec 31 2004.

[56] Suchitra E. Sebastian, Neil Harrison, and Gilbert G. Lonzarich. Towards resolution of the fermi surface in underdoped high-T-c superconductors. *Reports on Progress in Physics*, 75(10), Oct 2012.

[57] B. J. Ramshaw, James Day, Baptiste Vignolle, David LeBoeuf, P. Dosanjh, Cyril Proust, Louis Taillefer, Ruixing Liang, W. N. Hardy, and D. A. Bonn. Vortex lattice melting and H_{c2} in underdoped $YBa_2Cu_3O_y$. *Phys. Rev. B*, 86:174501, Nov 2012.

[58] M Von Zimmermann, JR Schneider, T Frello, NH Andersen, J Madsen, M Kall, HF Poulsen, R Liang, P Dosanjh, and WN Hardy. Oxygen-ordering superstructures in underdoped YBa(2)Cu(3)O(6+x) studied by hard x-ray diffraction. *Physical Review B*, 68(10):104515, Sep 1 2003.

[59] C Bergemann, AP Mackenzie, SR Julian, D Forsythe, and E Ohmichi. Quasi-two-dimensional fermi liquid properties of the unconventional superconductor Sr2RuO4. *Advances in Physics*, 52(7):639–725, Nov 2003.

[60] Alain Audouard, Cyril Jaudet, David Vignolles, Ruixing Liang, D. A. Bonn, W. N. Hardy, Louis Taillefer, and Cyril Proust. Multiple quantum oscillations in the $dehaas - vanalphen$ spectra of the underdoped high-temperature superconductor $YBa_2Cu_3O_{6.5}$. *Phys. Rev. Lett.*, 103:157003, Oct 2009.

[61] Suchitra E Sebastian, N Harrison, FF Balakirev, MM Altarawneh, PA Goddard, Ruixing Liang, DA Bonn, WN Hardy, and GG Lonzarich. Normal-state nodal electronic structure in underdoped high-Tc copper oxides. *Nature*, 2014.

[62] BJ Ramshaw. *Shubnikov-de Haas Measurements and the Spin Magnetic Moment of YBa2Cu3O6.59*. PhD thesis, Ph. D. thesis, University of British Columbia, 2012.

[63] T Graf, JD Thompson, MF Hundley, R Movshovich, Z Fisk, D Mandrus, RA Fisher, and NE Phillips. Comparison of CeRh2Si2 and CeRh2-xRuxSi2 near their magnetic-nonmagnetic boundaries. *Physical review letters*, 78(19):3769, 1997.

[64] RA Fisher, F Bouquet, NE Phillips, MF Hundley, PG Pagliuso, JL Sarrao, Z Fisk, and JD Thompson. Specific heat of CeRhIn5: Pressure-driven evolution of the ground state from antiferromagnetism to superconductivity. *Physical Review B*, 65(22):224509, 2002.

[65] M Nakashima, K Tabata, A Thamizhavel, TC Kobayashi, M Hedo, Y Uwatoko, K Shimizu, R Settai, and Y Ōnuki. High-pressure effect on the electronic state in CeNiGe3: pressure-induced superconductivity. *Journal of Physics: Condensed Matter*, 16(20):L255, 2004.

[66] Georg Knebel, Dai Aoki, Jean-Pascal Brison, and Jacques Flouquet. The quantum critical point in CeRhIn5: a resistivity study. *Journal of the Physical Society of Japan*, 77(11), 2008.

[67] Walter Kohn. Cyclotron resonance and de Haas-van Alphen oscillations of an interacting electron gas. *Phys. Rev.*, 123:1242–1244, Aug 1961.

[68] S Engelsberg and G Simpson. Influence of electron-phonon interactions on de Haas-Van Alphen effects. *Physical Review B*, 2(6):1657–&, 1970.

[69] D. A. Bonn, S. Kamal, Kuan Zhang, Ruixing Liang, D. J. Baar, E. Klein, and W. N. Hardy. Comparison of the influence of Ni and Zn impurities on the electromagnetic properties of $YBa_2Cu_3O_{6.95}$. *Phys. Rev. B*, 50:4051–4063, Aug 1994.